MDPI

*Review*

# Research Progress on Preparation of Superhydrophobic Surface and Its Application in the Field of Marine Engineering

Jingguo Fu [1], Xiaogang Liao [1], Yulong Ji [1,*], Yanqiang Mo [1] and Jifeng Zhang [1,2]

1   Department of Marine Engineering, Dalian Maritime University, Dalian 116026, China;
    fjingguo@dlmu.edu.cn (J.F.); lxg1120231149@dlmu.edu.cn (X.L.); muyanssar@163.com (Y.M.);
    zhangjifeng@dlmu.edu.cn (J.Z.)
2   Yangtze Delta Region Institute of Tsinghua University Zhejiang, Jiaxing 314006, China
*   Correspondence: jiyulong@dlmu.edu.cn; Tel.: +86-411-8472-4306

**Abstract:** Inspired by the "Lotus Leaf Effect" in nature, the phenomenon of superhydrophobia has attracted tremendous attention from researchers. Due to their special surface wettability, the superhydrophobic surfaces have been found to have broad potential applications in the fields of marine engineering, medical equipment, and aerospace. Based on the introduction of the principles of wettability, the advantages and disadvantages of various preparation methods for superhydrophobic surfaces were studied and summarized in this paper. The research progress on superhydrophobic surfaces in marine engineering applications was analyzed according to their self-cleaning, anti-corrosion, heat transfer, drag reduction, anti-fouling, ant-icing, and oil/water separation properties. Finally, to advance practical applications, the current challenges associated with superhydrophobic surfaces are highlighted, and potential future development directions are proposed.

**Keywords:** superhydrophobic surface; preparation methods; surface properties; research progress; marine engineering

## 1. Introduction

Wettability is an important characteristic of material surfaces. When a surface of the material comes into contact with the droplet, the phenomena of wetting, infiltration, and spreading will occur due to the different wetting properties. The static contact angle ($\theta$) between the liquid and solid phases is generally used to characterize the wettability of the material surface [1]. According to the value of the static contact angle, the surface wettability of the material can be classified as superhydrophilic, hydrophilic, hydrophobic, or superhydrophobic, and its static contact angles are $\theta < 5°$, $5° < \theta < 90°$, $90° < \theta < 150°$, and $\theta > 150°$, respectively. A surface with a static contact angle greater than $150°$ and a rolling contact angle less than $10°$ is defined as a superhydrophobic surface [2]. Due to their special surface-wetting properties, superhydrophobic surfaces have attracted wide attention from researchers, and it has been found that the special surface-wetting properties of the materials with self-cleaning [3,4], anti-fouling [5], corrosion resistance [6,7], drag reduction [8], anti-icing [9], and oil/water separation [10,11] properties have high potential applications in marine engineering, medical equipment, aerospace, and other fields.

Researchers first observed this superhydrophobic phenomenon in some natural plants and animals, such as lotus leaves [12,13], salvinia natans [14], water strider legs [15], and penguin feathers [16]. They found that the micro/nanoscale composite structures on the surface were key to their superhydrophobic properties, as shown in Figure 1. Based on these characteristics, artificial methods have been developed to manufacture bionic superhydrophobic surfaces, and their properties have been extensively studied [17,18]. These findings have brought the study of superhydrophobic surfaces to a new stage.
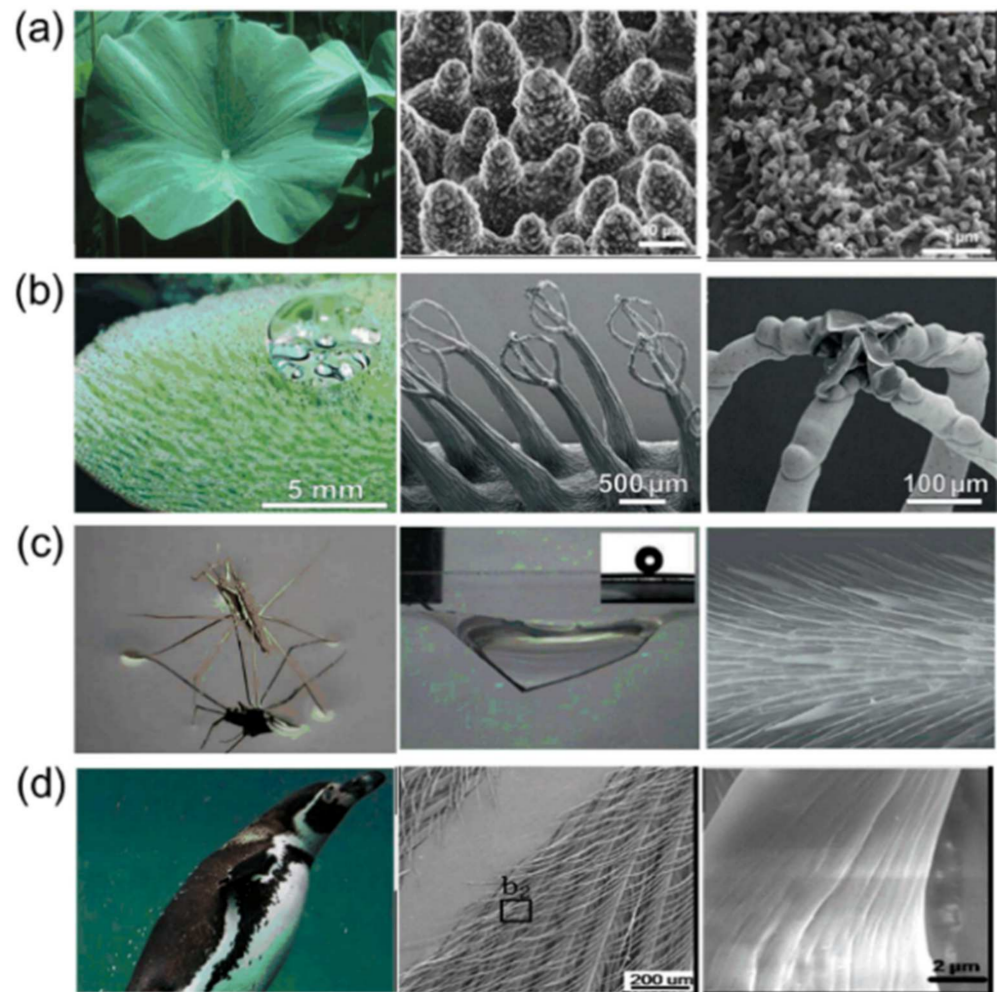
**Figure 1.** Typical plants and creatures: (**a**) lotus leaf [12], (**b**) salvinia natans [14], (**c**) strider leg [15], (**d**) penguin feather [16].

According to the search results of published papers from the Web of Science database (searching keyword: superhydrophobic), the study of the superhydrophobic phenomenon has received continuous attention since 2009. The number of related papers published on the topic of superhydrophobicity increased rapidly in 2011 and 2019. Moreover, over the past five years, the number of articles published each year is about 2000, as shown in Figure 2. Based on these data, the search results were classified according to performance-related keywords (such as self-cleaning and anti-corrosion), and the results showed that preliminary research mainly focused on the application of self-cleaning and anti-corrosion. Since 2015, the application of superhydrophobic surfaces for oil/water separation and anti-icing has gradually increased. Moreover, the number of papers concerning heat transfer and drag reduction has also increased significantly, indicating that it also has potential wide applications in these fields.

It can be seen that the research on superhydrophobic surfaces and their properties has been of great interest. In the past decades, the preparation of superhydrophobic surfaces has generally started from two aspects: the construction of binary micro-nano structures and the modification of low surface energy materials on the target surface. The commonly used methods to construct micro-nano structures are machine cutting [19], the hard-anodizing process [20], potassium hydroxide and lauric acid etching [21], ammonia etching [22], and high-speed wire EDM [23]. In terms of the modification of low surface energy, long-chain perfluorosilanes, such as 1H, 1H, 2H, 2H-perfluorodecyl triethoxysilane [22], cetyltrimethoxysilane [21], 1H, 1H, 2H, and 2H-perfluorooctane trichlorosilane [24], are generally selected.
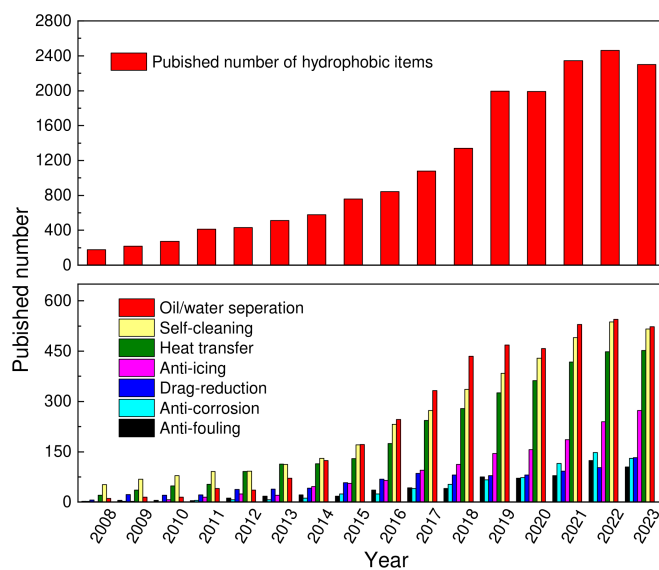
**Figure 2.** Statistical analysis of published SCI papers in the superhydrophobic field (data from the Web of Science database).

It is also well known that some materials have intrinsic water-repellency properties, such as polydimethylsiloxane (PDMS), and Polytetrafluoroethylene (PTFE). Thus, superhydrophobic surfaces can be obtained by fabricating micro/nanostructures directly on the surfaces of such materials. Zhang et al. [25] utilized a stainless steel plate with micro-nano structures as a template to directly fabricate PDMS superhydrophobic films featuring corresponding microstructures, which exhibited icing time 3.3 times longer. Meanwhile, Hsueh et al. [26] employed the low surface energy properties of PTFE to prepare a superhydrophobic surface with a hierarchical wrinkled micro-nano structure on a thermoretractable polystyrene (PS) sheet. The preparation methods are diverse and have different characteristics. The surfaces prepared by these methods all exhibit good superhydrophobicity.

However, it was also found that the disappearance of either of these two factors would lead to the weakening of superhydrophobic surface properties. The binary micro-nano structure of the superhydrophobic surface is easily damaged by external mechanical friction or collision, and the low surface energy on the surface also disappears after extended use. Consequently, the thin air film, known as the plastron, on the superhydrophobic surface is destroyed, and the superhydrophobic properties are lost. Therefore, researchers have begun to select superhydrophobic surfaces with different characteristics, based on various application scenarios. In a working environment where the micro-nano structure of the superhydrophobic surface is more likely to be damaged, such as water collection in dry areas, self-cleaning of solar panels, and anti-icing on aircraft, preparation methods with high mechanical durability are selected. In a working environment where the low surface energy material on the superhydrophobic surface is easily lost, such as heat transfer in the heat exchanger, drag reduction on the hull surface, oil/water separation, anti-corrosion, and anti-pollution on the surface of the underwater structure, preparation methods that allow the surface energy material to be slowly released are adopted.

Although there are ways to achieve both results at the same time, there are still some limitations in actual use. It is mainly reflected in the high cost, non-expandability, complex methods, or unadaptability of the substrate. In addition, long-chain perfluorosilanes are considered pollutants of high global concern due to their toxicity, resistance to degradation, and bioaccumulation [27]. For example, the commonly used low surface energy material stearic acid also has a low melting point, which may limit its application in heat exchangers and condensers operating in high-temperature environments. Octafluorocyclobutane is not only a greenhouse gas that destroys the ozone layer but also has certain toxicity and dangers. Perfluorooctane sulfonate is a persistent organic pollutant that is highly toxicity to aquatic organisms. However, it has extremely high stability and is difficult to

dissolve in the environment. After long-term use, these low surface energy substances gradually infiltrate the surrounding environment, and when accumulated to a certain extent, irreversible pollution occurs. These compounds have been detected in the environment, fish populations, and humans [28]. This is another key problem for superhydrophobic surfaces.

Marine engineering involves many equipment such as ocean vessels, offshore mobile or fixed building structures, underwater vehicles, deep sea, and polar equipment, and marine engineering occupies a large place in the industrial field. This field mainly studies technologies for marine energy saving, equipment corrosion protection, pollution prevention, anti-biological adhesion, and anti-icing. The superhydrophobic surface has performed excellently in these studies. However, when a superhydrophobic surface is applied in the field of marine engineering, the causes of its failure are significantly different from those in other fields, mainly reflected in the various working environments and special application requirements. For example, when applying a superhydrophobic surface to the hull surface for drag reduction, durability against water flow impact is required rather than mechanical durability against external hard objects. When a superhydrophobic surface is applied to offshore buildings, the corrosion resistance of salts in the environment and the adhesion of marine organisms in the ocean are needed, rather than the corrosion resistance of external acid and alkali and the antibacterial property. When a superhydrophobic surface is applied to polar equipment, the requirements for the anti-icing performance of deck equipment differ from the anti-icing performance of rarefied air in the aviation field. Although superhydrophobic surfaces have special application conditions in the field of marine engineering, there is a lack of a systematic summary of their application in this field.

Hence, in this paper, based on an introduction to the wetting principles of superhydrophobic surfaces, various preparation methods for superhydrophobic surfaces are reviewed. Their advantages and disadvantages were compared. The research progress in the application of superhydrophobic surfaces in the field of marine engineering was analyzed. Finally, the challenges and corresponding strategies for the application of superhydrophobic surfaces are discussed.

## 2. Basic Wetting Theories of Superhydrophobic Surface

The basic wetting theories of surfaces have been developed from the original Young's model [1] through the Wenzel model [29] to the present Cassie-Baxter model [30]. The static contact angle ($\theta$) was first proposed by Thomas Young in 1805, which reflects the result of the surface tension balance between solid, liquid, and gas interfaces and represents the triangular relationship between liquid surface tension and surface contact angle, as shown in Figure 3a. The equation is described as follows:

$$\gamma_{sg} = \gamma_{sl} + \gamma_{lg} \cos \theta_Y \tag{1}$$

where, $\gamma_{sg}$ is the interface tension between solid and air. $\gamma_{sl}$ is the interface tension between solid and liquid. $\gamma_{lg}$ is the interface tension between liquid and air. In Young's model, the solid surface is assumed to be a smooth ideal surface, and the influence of the surface roughness on the wetting state of the solid surface is ignored. Therefore, the Wenzel model was proposed after considering the surface roughness, where it is believed that the increase in roughness will make the actual contact area between the solid and liquid greater than the projected area of the solid–liquid contact surface, as shown in Figure 3b. The equation is described as follows:

$$\cos \theta_W = r \cos \theta_Y \tag{2}$$

where, $\theta_W$ is the contact angle of the droplet on a rough solid surface. $r$ is the ratio of the actual surface area to the projected area, which is usually greater than or equal to 1. As can be seen from Equation (2), the increase in the solid surface roughness will make the hydrophilic surface more hydrophilic and the hydrophobic surface more hydrophobic. However, Equation (2) still has its limitations. When a certain amount of air is enclosed in the micro-nano structure of the non-uniform surface, the actual contact area between

the droplet and the solid surface will change. Thus, the Wenzel equation is not applicable under such conditions.
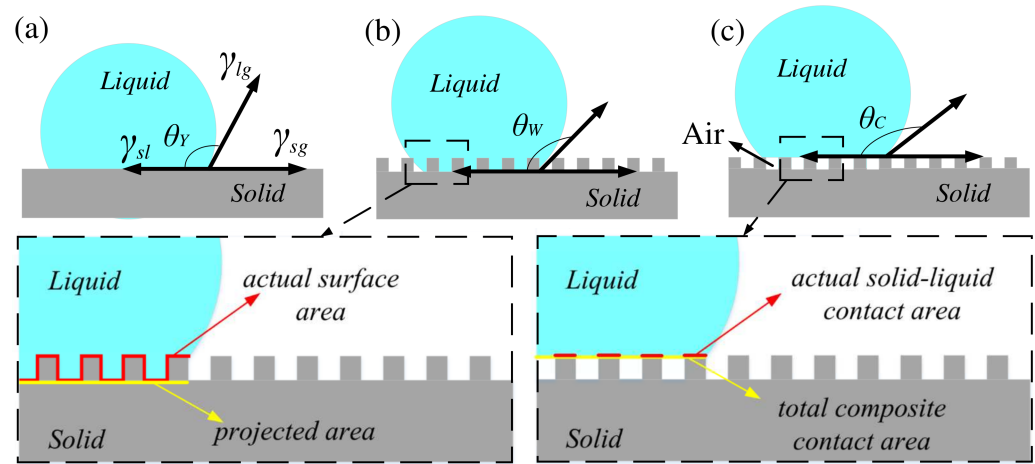


**Figure 3.** Schematic of a liquid droplet on a solid surface: (**a**) Young's model, (**b**) Wenzel model, (**c**) Cassie-Baxter model.

Therefore, Cassie and Baxter introduced the concept of phase area fraction ($f$) to quantitatively consider the effects of multiphase surfaces. The phase area fraction refers to the percentage of the total contact area of each phase on a non-uniform surface. To simplify the calculation process, it is assumed that the composite surface is composed of only two different multiphases, where the intrinsic contact angles of the droplet on each phase are $\theta_X$ and $\theta_Y$, and the percentages of each phase in the total area are $f_1$ and $f_2$. Thus,

$$f_1 + f_2 = 1 \tag{3}$$

Then, the Cassie and Baxter equation is described as follows:

$$\cos\theta_C = f_1 \cos\theta_X + f_2 \cos\theta_Y \tag{4}$$

However, if the surface is composed of solid and gas phases, the actual contact area of the droplet is comprised of two distinct parts. These are the contact area between the droplet and the solid, aa, and the contact area between the droplet and the air trapped in the groove, as shown in Figure 3c. The intrinsic contact angle between the droplet and the air is 180°, and the Cassie-Baxter equation is simplified as follows:

$$\cos\theta_C = -1 + f(\cos\theta_Y + 1) \tag{5}$$

where, $f$ is the percentage of the actual solid–liquid contact area to the total composite contact area. According to Equation (5), a larger contact angle can be achieved by regulating the microstructure of the solid surface and reducing the percentage of the solid–liquid contact area in the total contact area.

However, it has also been proven that the simplified Cassie-Baxter equation is correct for the case of smooth-topped pillar geometries with coplanar solid–liquid and liquid–vapor interfaces (for zero penetration of liquid). In general, for an arbitrary rough surface, such as equilateral pyramid-topped square pillars, conical pillars, discrete spherical particles, and surface structures with various re-entrant curvatures, have emerged [31,32], the original form of the Cassie-Baxter Equation (4) should be used, in which the value of

$$f_1 \neq f, \ f_2 \neq 1 - f, \ f_1 + f_2 > 1 \tag{6}$$

where, $f_1$ and $f_2$ can both be greater than unity.

Furthermore, the droplet completely infiltrates the concave and convex structures of the rough surface in the Wenzel model, making the droplet adhere to the surface and difficult to roll off. While, in the Cassie-Baxter model, the droplet is suspended on a rough surface. Since only part of the solid surface is in contact with the droplet, it is prone to rolling off. These theoretical explanations are consistent with natural or laboratory phenomena, so the Cassie-Baxter model is also the most accepted by researchers. However, the unique environmental factors of marine environments, such as high humidity, high salinity fog, high/low temperature, intense illumination, and continuous erosion by water currents, may lead to the degradation of the micro-nano structures on superhydrophobic surfaces or the gradual disappearance of low surface energy materials. This will lead to changes in the surface roughness ($r$) of the superhydrophobic surface as well as the percentage of the actual solid–liquid contact area to the total composite contact area ($f$), which ultimately affects the stability of the plastron on the superhydrophobic surface.

These alterations could precipitate a transition in the wetting state of superhydrophobic surfaces from the Cassie-Baxter state to the Wenzel state, thereby constraining their application potential in the field of marine engineering.

Moreover, in the investigation of practical applications of superhydrophobic surfaces, it is imperative to consider not only the static contact angle but also the advancing contact angle ($\theta_{adv}$) and the receding contact angle ($\theta_{rec}$) of water droplets on the surface. The sliding angle is one of the critical criteria for assessing the superhydrophobicity of a surface. On an ideal smooth surface, the wetting system tends toward an equilibrium state, where the droplet exhibits a single contact angle. Conversely, on rough or chemically heterogeneous surfaces, the wetting phenomenon may exhibit metastability, leading to a range of contact angles for the droplet. The maximum and minimum values within this range are referred to as the advancing contact angle and the receding contact angle, respectively, as shown in Figure 4a,b. Contact angle hysteresis, typically defined as the difference between the advancing and receding contact angles, quantifies the degree of hesitation of a water droplet on a solid surface, and is related to factors such as adhesive hysteresis, surface roughness, and surface heterogeneity. The magnitude of the contact angle hysteresis is directly related to the sliding angle: a smaller sliding angle correlates with a smaller contact angle hysteresis, while a larger sliding angle corresponds to a larger contact angle hysteresis.
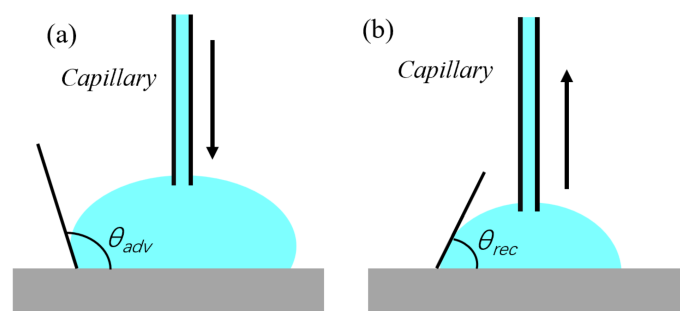


**Figure 4.** Schematics for measuring advancing and receding contact angles: (**a**) the advancing contact angle, (**b**) and the receding contact angle.

## 3. Preparation Methods of Superhydrophobic Surfaces

According to a study of the superhydrophobic phenomenon and wetting theories of natural plants and animals, it was found that constructing a binary micro-nano structure and the modification of low surface energy materials on the target surface are the key ways to prepare superhydrophobic surfaces [33]. Currently, the preparation methods for superhydrophobic surfaces mainly include the template method, etching method, spraying method, and electrochemical method.

### 3.1. Template Method

The template method uses a substrate with a certain regular or irregular binary micro-nano structure as the template, and the casting mold is uniformly coated [34] or pressed [35] on the template. A rough surface opposite to the micro-nano structure of the template can be prepared after stripping, and then a superhydrophobic surface can be prepared after modification by low surface energy materials. Currently, many kinds of materials can be used as templates, including soft materials, such as lotus leaves [36], taro leaves [37], and polyethylene glycol [38], and hard materials, such as metal and its oxide [24]. Peng et al. [37] used taro leaves as a template to prepare a polydimethylsiloxane superhydrophobic surface with a surface contact angle of up to 154° and a rolling contact angle of less than 4°, as shown in Figure 5a. Wang et al. [39] fabricated the armored structures on metal substrates using silicon micro-pyramid arrays via cold pressing technology, as shown in Figure 5b.
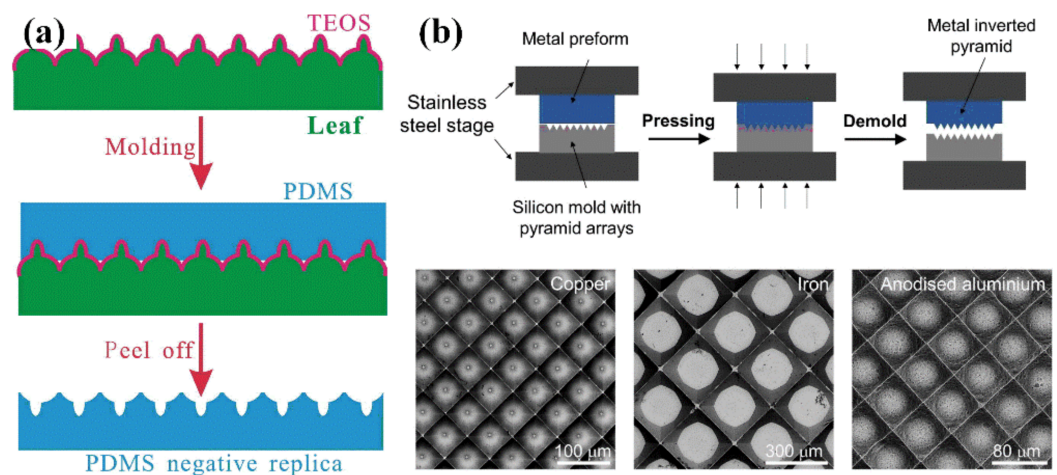


**Figure 5.** Template method: (**a**) soft template [37], (**b**) hard template [39].

The aforementioned studies demonstrated that the template method offers a relatively direct fabrication process, enabling the formation of the requisite micro-nanostructures through a facile replication procedure, which is easily controllable. This attribute is of particular significance for scenarios in marine engineering that necessitate the mass production of superhydrophobic surfaces. Moreover, the template method can be applied to a diverse array of materials, encompassing polymers and glass, thereby endowing it with extensive potential for application within the realm of ocean engineering. Furthermore, by selecting templates with varying shapes and structural configurations, the topography of the superhydrophobic surface can be meticulously controlled, ensuring the uniformity and reproducibility of the superhydrophobic surfaces. This adaptability endows the template method with the capability of catering to a multitude of ocean engineering applications, thereby satisfying a spectrum of requirements. However, the template method necessitates the fabrication of high-precision templates and the execution of sophisticated processing techniques, which impose stringent demands on equipment and technological proficiency. These requirements may impose limitations on large area fabrication, potentially restricting their application to large-scale marine structures. Additionally, the risk of template damage during the fabrication process is an inherent concern, and the selection of template materials emerges as a critical factor that warrants careful consideration.

### 3.2. Etching Method

The etching method refers to the construction of binary micro-nano structures directly on a solid surface by chemical or physical methods, which are then modified with low surface energy materials to prepare a superhydrophobic surface. At present, the more commonly used etching methods are chemical etching [40], mechanical etching [41], laser etching [42], and plasma etching [43]. Zhang et al. [44] prepared a superhydrophobic surface

with a micro-nano hierarchical structure on the surface of 5083 aluminum alloy by etching with ammonia water and modifying with 1H, 1H, 2H, 2H-perfluorodecyl triethoxysilane (PFDTES), as shown in Figure 6a. Compared with aluminum alloy, the corrosion resistance of the prepared superhydrophobic surface was improved by three orders of magnitude in the simulated marine environment, and the adhesion rate of Sulfate-Reducing Bacteria (SRB) decreased by 93.77% after 6 days of immersion in sulfate-resistant reducing bacteria (SRB) medium. Zhu et al. [45] designed the superhydrophobic surface on the aluminum alloy surface utilizing the mechanical lathe cutting method and stearic acid modification. It was found that the forward speed and tilt angle of the milling cutter had a great influence on the wettability of the superhydrophobic surface, as shown in Figure 6b.
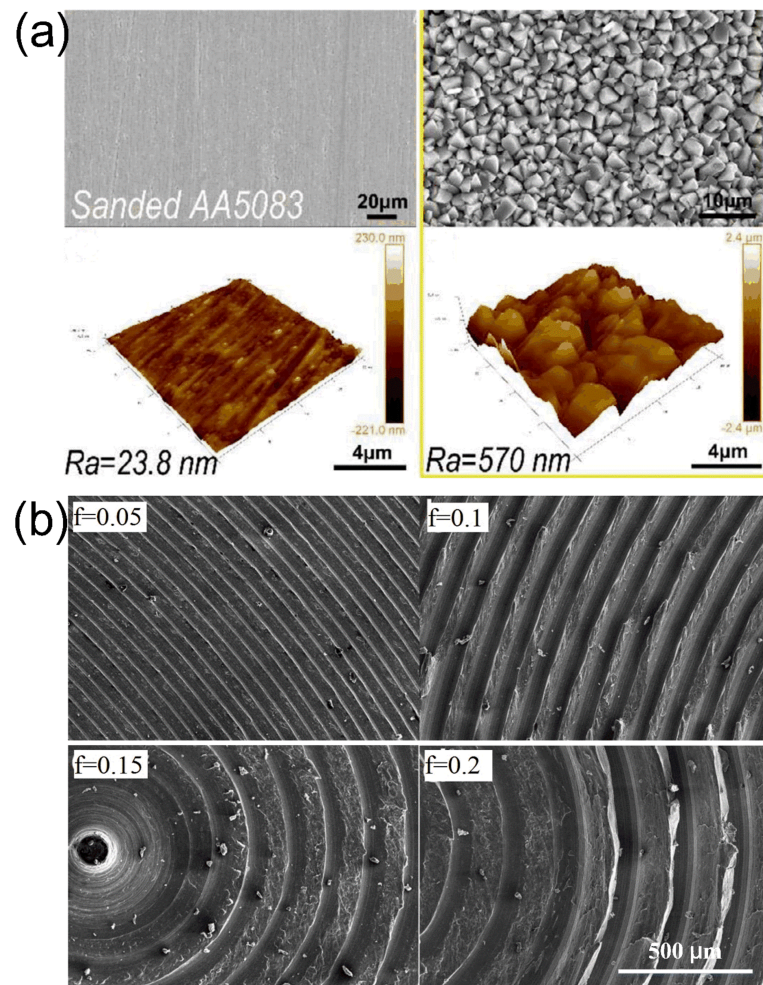


**Figure 6.** Etching method: (**a**) chemical etching: SEM and AFM images of sanded AA5083 and superhydrophobic AA5083 surface [42], (**b**) mechanical etching: SEM of the as-prepared surfaces with different forward speeds and tilt angles [43].

Thus, the etching method is applicable to various materials, encompassing metals and ceramics. This offers flexible selection to cater to the diverse requirements of marine engineering structures. Moreover, the etching method allows precise control over the dimensions and morphology of the surface microstructures, and the surfaces must be machined one point at a time, which is crucial for achieving the desired superhydrophobic properties. For instance, mechanical etching, laser etching, and plasma etching are usually utilized. However, the etching method may necessitate costly equipment and intricate procedural steps, demanding a high level of technical proficiency to accurately control the etching conditions and thereby obtain the optimal surface architecture. This can lead to increased costs, particularly in large-scale production scenarios. Some etching methods,

like acid etching, may generate harmful effluents and exhaust gases during the etching process, posing environmental pollution risks and necessitating consideration of health hazards to operating personnel. These drawbacks may limit the rapid dissemination and application of etching techniques in marine engineering.

### 3.3. Electrochemical Method

The electrochemical method involves the formation of a superhydrophobic metal surface via the redox reaction of cations and anions in solution under the action of an applied electric field. There are many kinds of electrochemical methods. Special micro-nano structures of metal particles such as silver, nickel, or copper can be fabricated on metal surfaces via electroplating [46] or electrochemical deposition [47] methods. Then, the surfaces are modified with low surface energy materials to prepare superhydrophobic surfaces with high self-cleaning and corrosion resistance. Some researchers have also used anodic oxidation [48] or micro-arc oxidation [49] methods to obtain a binary micro-nano structure on a valve metal surface and obtain a superhydrophobic surface after treatment with low surface energy materials. The superhydrophobic surface structures prepared by these methods (as shown in Figure 7) are relatively uniform. However, these coatings are thinner and less durable. With the continuous development of these technologies, some composite technologies have been adopted to prepare superhydrophobic surfaces and have become a current research hotspot, such as micro-arc oxidation combined with electrodeposition [50] and micro-arc oxidation combined with the hydrothermal method [51].
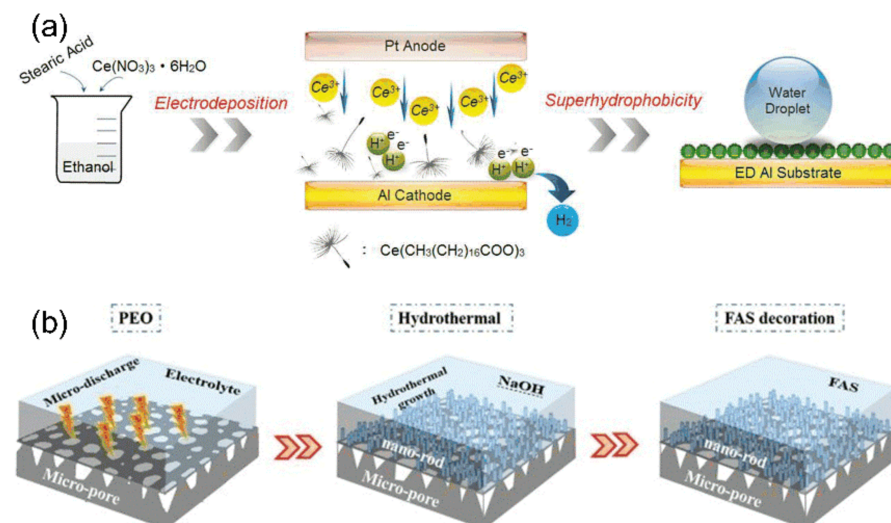


**Figure 7.** Electrochemical method: (**a**) electrodeposition: schematic of nonfluorinated one-step fabrication of superhydrophobic [47], (**b**) PEO + Hydrothermal: schematic illustration of the sample preparation process [51].

For these kinds of electrochemical methods, the microporous ceramic layer produced by micro-arc oxidation increases the matrix strength and the bonding strength with the outer superhydrophobic coating. Thus, its durability is greatly improved. Furthermore, after the composite process, the number of micro-pores obtained by micro-arc oxidation on the metal surface is also reduced, reducing the entry of corrosive media and further enhancing the anti-corrosion performance of the superhydrophobic surface. However, in the existing literature, this method has not been applied to full-scale industrial production, which may be related to the parameters and efficiency of the electrochemical process.

### 3.4. Spraying Method

The spraying method uses spraying equipment to spray the mixed solution containing modified micro-nano particles directly onto the surface. In addition, to improve the bonding strength of the spraying coating, a layer of adhesive is sprayed first, or the mixed solution

is generally mixed with the adhesive. For example, Wang et al. [52] dispersed stearic acid-modified ZnO nanoparticles in a mixed solution of epoxy resin and fluorinated ethylene propylene and sprayed the mixture onto the surface of aluminum with a certain roughness to produce a superhydrophobic surface with a contact angle of 160°, as shown in Figure 8a. Xie et al. [53] sprayed modified nano-silicon particle solution on the surface of semi-cured alkyd resin and polypropylene. Xin et al. [54] sprayed stearic acid-modified $SiO_2$ and $TiO_2$ micro-nano particle solution on the surface of semi-cured epoxy resin. A superhydrophobic surface could be formed after this resin curing. Based on this, Cao et al. [55] established a method of constructing a superhydrophobic surface that was suitable for almost any micro-nano particles using polydimethylsiloxane as a medium. The particles were directly sprayed onto the polydimethylsiloxane layer, which solved the problem of dispersibility of the modified particles in the mixed solution. Moreover, according to the different properties of modified micro-nano particles, a variety of thermal coating, conductive coating, and catalytic coating can be prepared, as shown in Figure 8b.
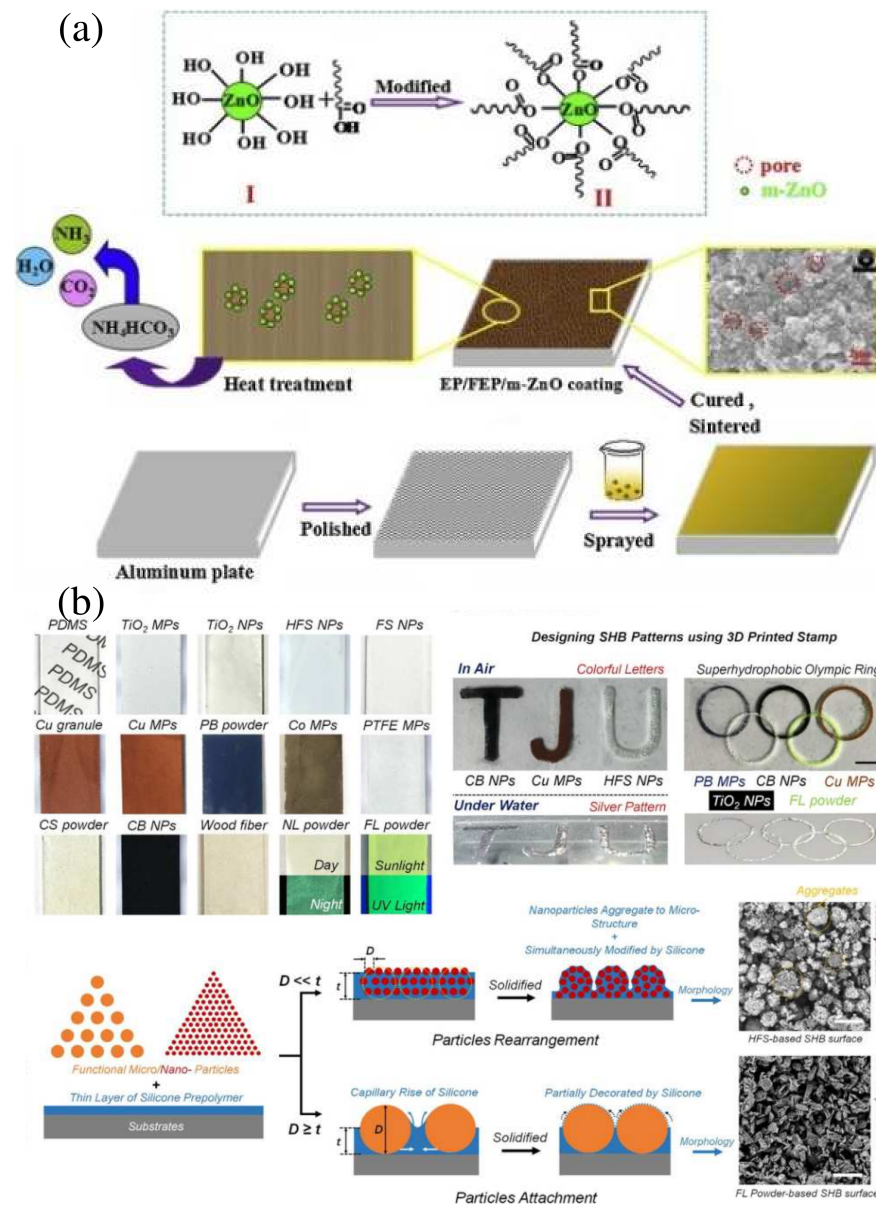


**Figure 8.** Spraying method; (**a**) direct spraying: schematic sketch of the main procedure of coating fabrication [52], (**b**) glue + powder: optical photos of prepared superhydrophobic surfaces on glass slides, and the selected particles including metallic powder, metal oxide, and organics [55].

Because of its simple and economical characteristics and its ability to be not limited by the size and shape of the solid surface, this type of method can be used to prepare superhydrophobic surfaces over a large area with a wide range of potential applications. However, the bonding strength of the coating and the substrate is a key factor restricting the durability of the superhydrophobic surface. In addition, the dispersion of the modified micro-nano particles in the mixed solution has a great influence on the wettability of the coating.

### 3.5. Other Methods

In addition to the above preparation methods, other methods have also been considered by other researchers to increase the applicability of a variety of substrates. For example, the sol−gel method [56] was adopted to fabricate a superhydrophobic surface by depositing $Al_2O_3$ nanoparticles on a copper surface. The electrospinning method [57] was employed to prepare a polyvinylidene fluoride (PVDF)/stearic acid nanofiber superhydrophobic coating on the metal surface. 3D printing technology [58] was used to fabricate a biomimetic sophora japonica superhydrophobic surface. The powder pressing method [59] was adopted to press silica powder on the surface of the semi-cured silica gel to form a superhydrophobic surface. Furthermore, a one-step photopatterning method was adopted to obtain a two-layer polymer structure that exhibited excellent wettability and high light transmittance properties [60].

All of the above methods can be used to prepare superhydrophobic surfaces with good properties, but they still have their advantages and disadvantages. The detailed information is shown in Table 1.

**Table 1.** Advantages and disadvantages with regard to superhydrophobic surfaces by different preparations.

| Prepare Methods | | Low Surface Energy Substance | Advantages | Disadvantages | Ref. |
|---|---|---|---|---|---|
| Template methods | Hard template method | 1H, 1H, 2H, 2H-perfluorooctyl | Low cost and simple preparation | Poor mechanical durability, resistance to degradation | [35] |
| | Soft template method | PDMS | Low cost and simple preparation and high mechanical elongation | Poor mechanical durability | [38] |
| Etching methods | Chemical etching | 1H, 1H, 2H, 2H-Perfluorooctanesulfonic acid | Fast and simple preparation | Uncontrollable microstructure size and environmental pollution, resistance to degradation | [40] |
| | Mechanical etching | Stearic acid (SA) | Controllable microstructure size, Low cost | Requires special equipment and higher cost, bioaccumulation | [41] |
| | Laser micro-machining | Octafluorocycloboutane | Controllable microstructure size, Low cost | Requires special equipment and higher cost, high energy consumption, resistance to degradation | [42] |
| Electrochemical methods | Electroplating | Stearic acid (SA) | Simple and controllable preparation | Time-consuming, limited to small areas, and environmental pollution | [46] |
| | Electrochemical deposition | Stearic acid (SA) | Controllable reaction process | Small bonding force and limited to small areas | [47] |
| | Anodizing | Stearic acid (SA) | Simple and controllable preparation, Low cost | Time-consuming, limited applicable substrates, and environmental pollution | [48] |
| | Micro-arc oxidation (MAO) | Stearic acid (SA) | Fast and controllable preparation | Limited applicable substrates and high energy consumption | [49] |
| Spraying methods | Direct spraying | Stearic acid (SA) | Simple and applicable to different substrates and shapes, Low cost | Poor mechanical durability | [52] |
| | Glue + powder | Stearic acid (SA), fluorinated ethylene propylene (FEP) | Simple, applicable to different substrates and well-distributed particles | Poor mechanical durability | [55] |
| Any other methods | Sol−gel technique | PDMS | Simple reaction process and well distribution, Low cost | Time-consuming and environmental pollution | [56] |
| | Electrospinning | Stearic acid | Controllable microstructure size | Needed complex operations, high cost | [57] |

## 4. Application of Superhydrophobic Surface in Marine Engineering

*4.1. Application in Self-Cleaning*

As can be seen from Figure 2, the self-cleaning property has always been a research hotspot for superhydrophobic surfaces. In the field of marine engineering, there is an urgent need to remove salt particles from the ship surface to reduce the corrosion of deck equipment and to clean the high-viscosity crude oil or sludge attached to the wall of the oil tank to reduce the workload of crews. Due to the extreme non-wettability and the lower surface adsorption force of superhydrophobic surfaces, when droplets or viscous liquids come into contact with the superhydrophobic surface, the droplets form a spherical shape and roll off the surface, and the viscous liquids slide off the surface directly under the action of gravity. The contaminants on the surface can be carried away during rolling or sliding movements [61–63].

Hence, the self-cleaning performance of the superhydrophobic surface was tested by washing the solid particles scattered on the surface with droplets [64], as shown in Figure 9a. At present, the commonly used particles are black carbon [65,66], dust [67], and metal particles [68]. The prepared superhydrophobic surfaces showed superior self-cleaning properties. However, there are relatively few studies on the self-cleaning properties of viscous liquids. During the transportation of crude oil by marine vessels, the viscous crude oil adheres to the surfaces of the cargo holds, necessitating substantial labor and resources for their subsequent cleaning. Sticky artificial materials were used to test the self-cleaning performance of the superhydrophobic surface, which was prepared by spraying dimethyldimethoxysilane and silicone oil onto the nanostructured surface [69]. The results showed that the surface exhibited a super-strong self-cleaning effect on the viscous liquids, and the adhesion of the prepared surface could be reduced by 90% compared with the untreated surface, as shown in Figure 9b. However, the life of the superhydrophobic surface could only use about 50 flushing cycles, which is worse than that of some of the other surfaces tested, such as SLIPS and LESS. Su et al. [70] also adopted the same strategy and prepared a mixture of plastic and hydrophobic sand particles into a toilet model via laser 3D printing technology and then sprayed silicone oil on the surface. The prepared surface also exhibited excellent repulsion to complex fluids, such as artificial feces, yogurt, honey, and starch gels. However, when the surface silicone oil is exhausted, it must be repeatedly sprayed to restore its excellent superhydrophobic properties.
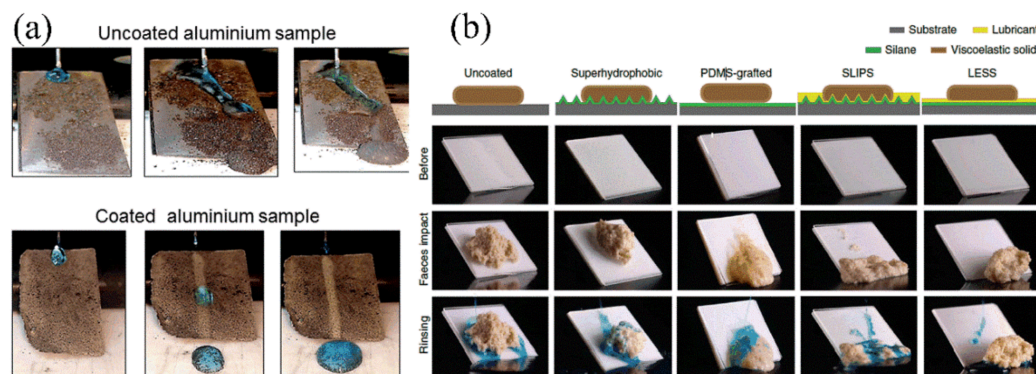


**Figure 9.** Self-cleaning property test: (**a**) flushing powder test: Optical images of self-cleaning behavior of as-received uncoated and superhydrophobic aluminum surfaces [64], (**b**) flushing viscous solid test: Schematic and optical images showing the comparison of adhesion between viscoelastic solids and different engineered surfaces [69].

For the application of superhydrophobic surfaces for self-cleaning purposes in the field of marine engineering, it is necessary to contend with prolonged frictional contact with cargoes such as coal and mineral sands during the transportation process. This necessitates that superhydrophobic surfaces possess enhanced mechanical durability, particularly for

hull surfaces obtained by spraying methods. However, it can be seen that the durability of superhydrophobic coatings is still a bottleneck for their application.

### 4.2. Application in Anti-Corrosion

Corrosion is one of the most common and unavoidable forms of failure in equipment in the field of marine engineering. According to the Cassie−Baxter model, when the superhydrophobic surface is in contact with a corrosive solution, due to its unique surface structure, a plastron will be formed between the superhydrophobic surface and the corrosive solution. The plastron will reduce the contact area between the substrate and the corrosive medium, thereby reducing the migration of corrosive ions and the corrosion rate of the substrate [71]. Thus, superhydrophobic surfaces can provide effective corrosion protection for engineering materials, such as aluminum [72], magnesium [73], and steel [74], especially in marine environments.

Zhang et al. [75] fabricated a manganese stearate superhydrophobic surface with a surface contact angle of 169.7° on a pure aluminum surface by one-step electrodeposition. The electrochemical impedance spectroscopy results showed that the contact impedance value improved by five orders of magnitude, and the corrosion current density decreased by four orders of magnitude. Furthermore, the superhydrophobic surface also showed good stability under acidic and alkaline conditions, as shown in Figure 10a,b. Some studies [50] have shown that the surface contact angle of the superhydrophobic surface can be decreased from 153.5° to 128.0° when immersed in a 3.5% NaCl solution for 85 h, indicating the disappearance of the Cassie-Baxter phenomenon on the superhydrophobic surface. Some studies [76] have even immersed the prepared superhydrophobic surface in solutions with different pH values to test its corrosion resistance. However, the retention time of the superhydrophobic properties was relatively short. Wu et al. [77] prepared an environmentally friendly superhydrophobic coating by combining modified expanded graphite (EAG) doped nano zinc oxide (ZnO) in epoxy resin. This fluorine-free superhydrophobic coating could last for 21 days in a neutral salt spray test, as shown in Figure 10c.

These results show that the long-term stability of the superhydrophobic surface is relatively poor in a salty environment and even worse under strong acid and alkaline conditions. In addition, the use of poly-fluorinated low-surface energy materials has also aggravated environmental pollution. Therefore, the focus of future research is on how to improve durability under extreme conditions and develop environmentally friendly superhydrophobic surfaces.

### 4.3. Application in Heat Transfer

Heat exchangers and condensers are widely used in the field of marine engineering, such as freshwater coolers, oil coolers, boiler condensers, and air conditioning condensers. The improvement in their performance is of great significance in enhancing the thermal efficiency of ships. The application of superhydrophobic surfaces in heat transfer is mainly reflected in two aspects, which are boiling heat transfer and condensation heat transfer. The large latent heat of the working fluid is utilized by boiling heat transfer. Steam bubbles are easily formed on the superhydrophobic surface under low superheat conditions and quickly detach away, increasing the heat transfer coefficient. During the condensation heat transfer process, micro-scale liquid droplets are easily formed on the superhydrophobic surface under low subcooling and quickly bounce or slide away under the action of gravity, increasing the heat transfer performance of condensation.

As for boiling heat transfer, Jo et al. [78] found that after bubbles are formed and detached from the heated hydrophobic surface, a small bubble will remain as the nucleation point for the next bubble growth, which is conducive to the rapid formation and detachment of the next bubble. Therefore, a hydrophobic surface provides better nuclear-boiling heat transfer than a hydrophilic surface. However, the boiling heat transfer performance of the hydrophobic surface is worse than that of the hydrophilic surface at high superheat, as shown in Figure 11a. Betz et al. [79] studied the influence of surface wettability on the

number of nucleation sites and found that under low superheat conditions, the number of nucleation sites on a superhydrophobic surface was greater than those on hydrophobic, hydrophilic, and superhydrophilic surfaces. Thus, nuclear boiling is more likely to occur on superhydrophobic surfaces. Vakarelski et al. [80] found that the hydrophobic surface was more likely to form bubbles than the superhydrophilic and hydrophilic surfaces, while the superhydrophobic surface produced a vapor layer, forming a film boiling heat transfer state, as shown in Figure 11b,c. These findings were also consistent with the results in references [81,82].
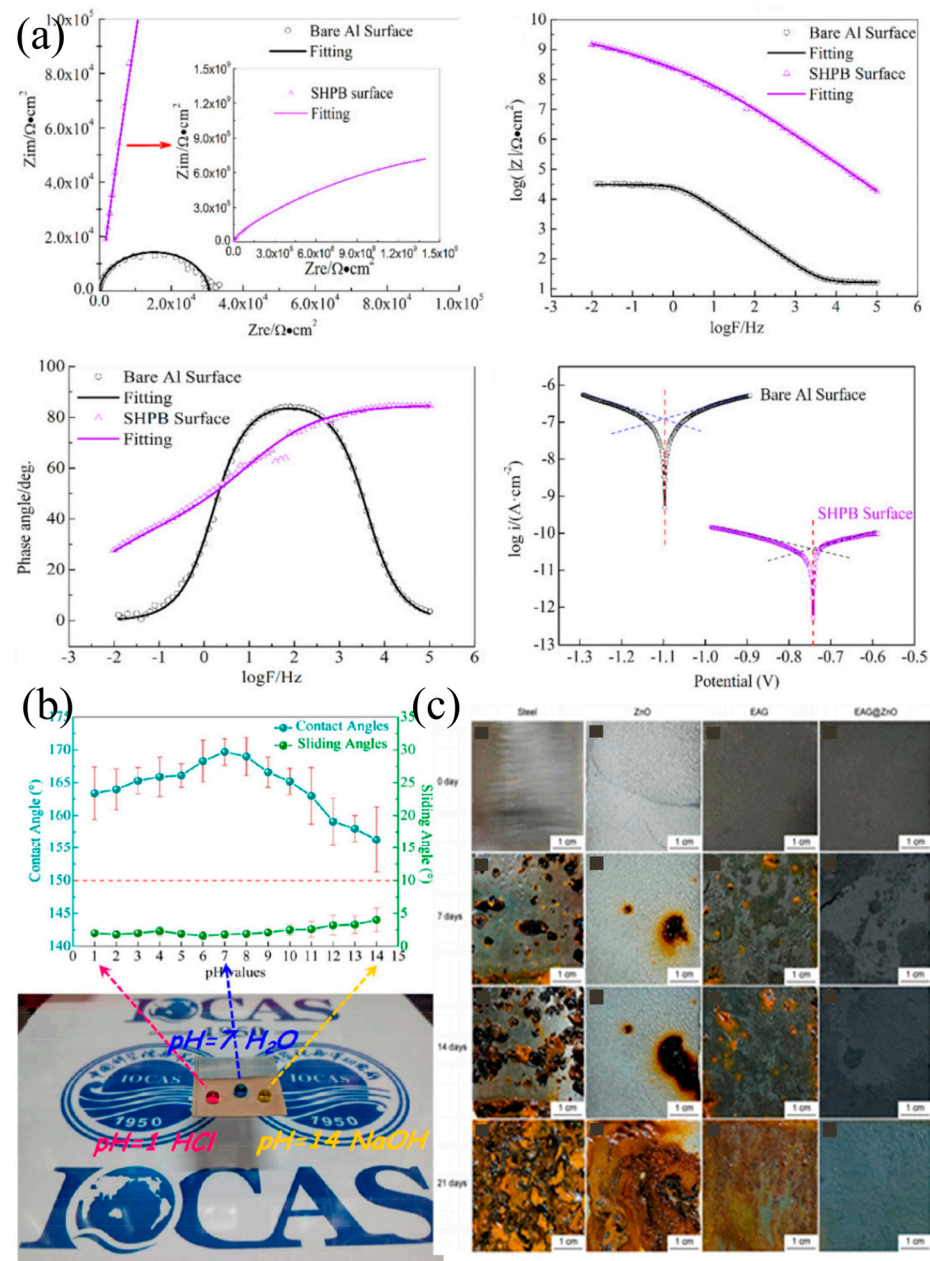


**Figure 10.** Anti-corrosion property test: (**a**) EIS and potentiodynamic polarization test [75], (**b**) Chemical stability test: Variation in the water contact angles of the synthetic SHPB surface as a function of pH values, photo of water droplets dyed with methylene blue and methyl red [75], (**c**) Exposure to salt spray chamber for different times [77].
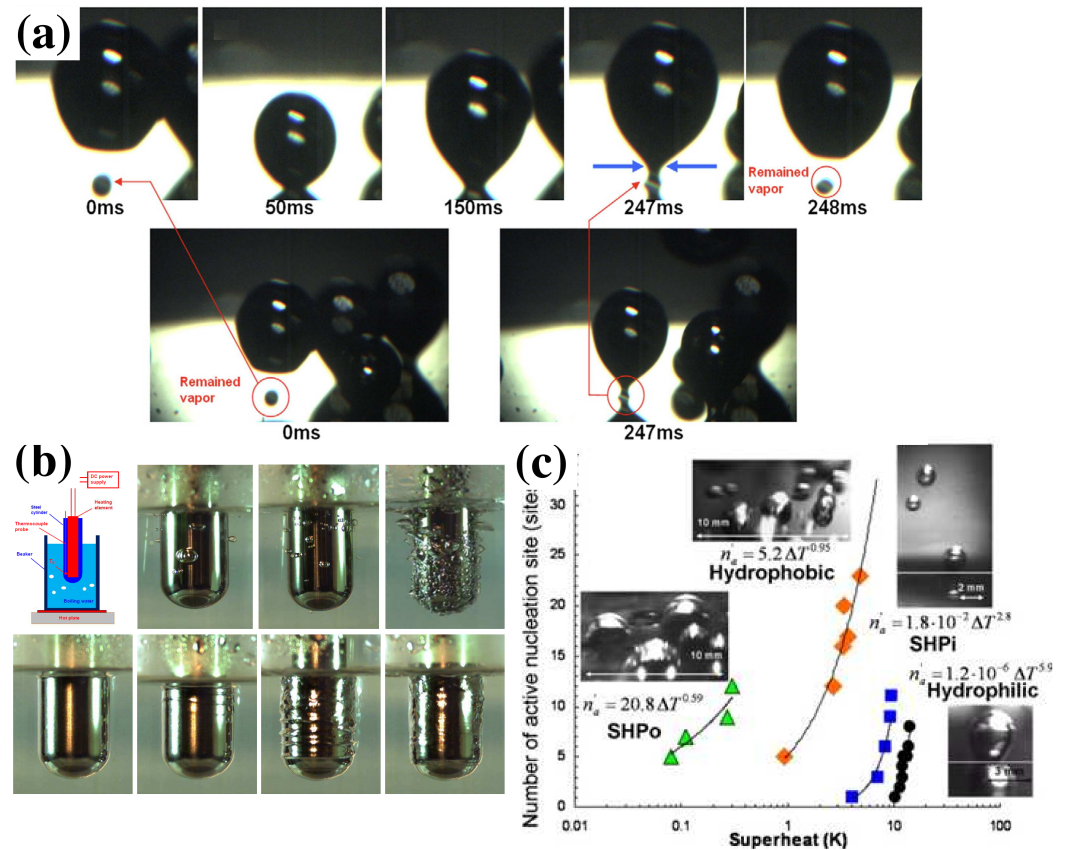
**Figure 11.** Effect of surface wettability on boiling heat transfer: (**a**) bubble detaching process [78], (**b**,**c**) boiling state on different surfaces: measured density of active nucleation sites for hydrophilic, hydrophobic, SHPi, and SHPo surfaces [80].

Regarding condensation heat transfer, Nenad et al. [83,84] studied the condensation heat transfer performance of copper tubes with different wettabilities. The results showed that at low supersaturations (S = 1.08), the steam condensed and formed a thin liquid film on the surface of the superhydrophilic copper tube, while a large number of micro-scale liquid droplets were formed, coalesced, and jumped away from the surface of the superhydrophobic copper tube, which was called dropwise condensation, as shown in Figure 12a. The condensation heat transfer coefficient increased by 40%. However, with the increase in supersaturation (S = 1.54), overflow condensation occurred on the superhydrophobic surface, resulting in a decrease in the condensation heat transfer performance. Furthermore, Zhang et al. [85] found that in the presence of a non-condensable gas, surfaces with different wettabilities showed similar results in reference [76]. Moreover, with an increase in the concentration of non-condensable gas in the environment, the intensity of droplet jumping gradually weakened, and the droplet jumping phenomenon was rarely observed at a concentration of 27.8%, as shown in Figure 12b,c. Based on these results, Khatir et al. [86] theoretically analyzed the phenomenon of coalescence and jumping of droplets on superhydrophobic surfaces via 2D lattice Boltzmann and 3D fluid volume methods. Additionally, Hao et al. [87] applied dropwise condensation of a superhydrophobic surface on an oscillating heat pipe (OHP) and found that the droplet movement path in the microchannel can be changed during the droplet jump, thus enhancing the heat transfer coefficient.
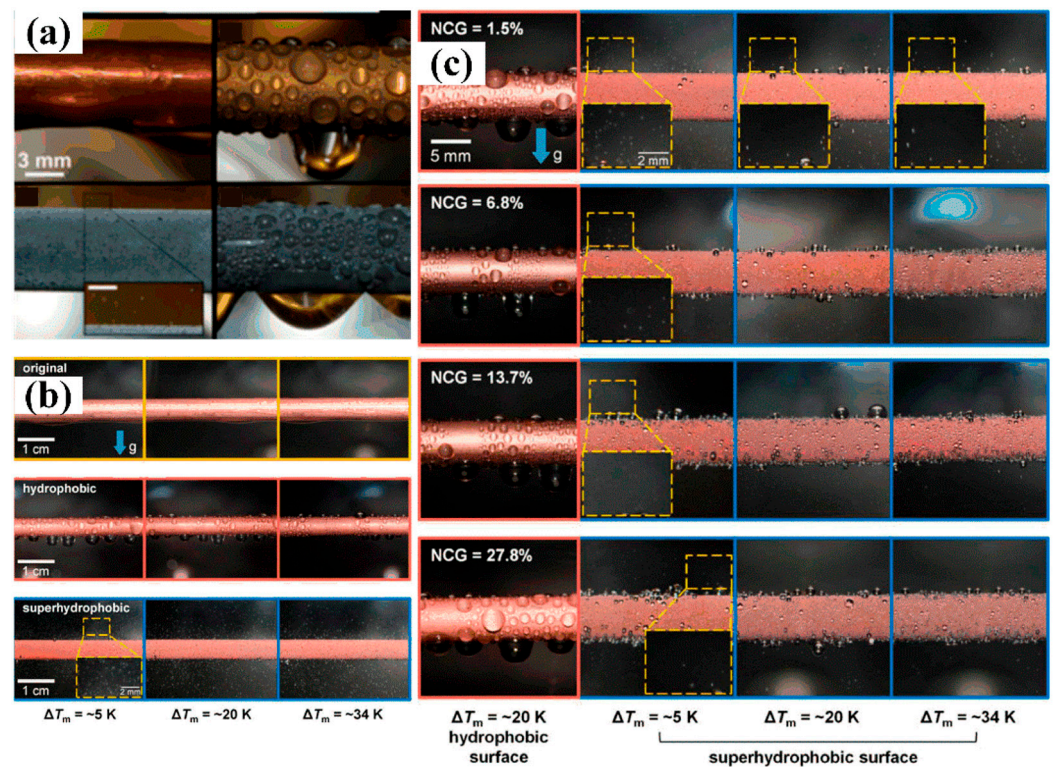
**Figure 12.** Effect of surface wettability on condensation heat transfer: (**a**) condensation state on different surfaces [84], (**b**,**c**) condensation state in different concentrations of non-condensable gas [85].

It can be seen that the boiling heat transfer performance at low superheats and condensing heat transfer performance at low supercooling of the superhydrophobic surface was better than that of hydrophobic, hydrophilic, and superhydrophilic surfaces. However, with the increase in superheat, the superhydrophobic surface is more likely to transition from nuclear boiling to film boiling, resulting in a decrease in boiling heat transfer performance. With the increase in supercooling, the superhydrophobic surface is more easily transformed from dropwise condensation to overflow condensation, resulting in a decrease in condensation heat transfer performance. Therefore, the application of superhydrophobic surfaces in heat transfer is suitable for situations with low superheat and low subcooling.

### 4.4. Application in Fluid Drag Reduction

If a superhydrophobic coating is applied to the outer surface of the hull, it can also reduce ship resistance. The viscous resistance generated by the hull and external liquid is a large part of the ship resistance. However, due to the appearance of the plastron on the superhydrophobic surface, the viscous resistance between the hull and the liquid is transformed into the viscous resistance between the gas and the liquid, which greatly reduces the value of viscous resistance, and then the fluid drag reduction effect appears [88,89]. Compared with the strategy of injecting bubbles [90,91], drag reduction of the superhydrophobic surface does not require additional external energy. Therefore, the use of a superhydrophobic surface to reduce ship resistance is one of the most important strategies for reducing energy consumption and efficiency.

In the experimental aspect, Zhang et al. [92] prepared the superhydrophobic surface on anodized aluminum via the hydrothermal method and 1H, 1H, 2H, 2H-perfluorooctadecyltrichlorosilane modification. Through the test of the liquid/solid surface drag experimental device, the surface drag value of the superhydrophobic surface was reduced by 20–30%, as shown in Figure 13a. Moreover, the drag reduction effect of the superhydrophobic surface has been verified by the steel ball falling test [93], two-dimensional particle image velocimetry (PIV) method [94], and spinning disk test [95].

However, the forms of these testing methods were different from the actual motion state of the ship. Therefore, Zhang et al. [96] prepared a composite superhydrophobic coating of polydimethylsiloxane (PDMS) and copper particles on the surface of the submarine model by the spraying method and found that the speed of the submarine model with superhydrophobic coating in the small pool was 15% higher than that of the ordinary model, as shown in Figure 13b. Meanwhile, Zhao et al. [97] studied the drag reduction performance of the superhydrophobic coating on a ship model by measuring the speed trend over time under different drag forces. Xin et al. [54] sprayed nano-$SiO_2$ polymer superhydrophobic coating on a small ship model and verified that the superhydrophobic coating can not only reduce the ship resistance (drag reduction rate ~ 30.09%) but also increase the ship buoyancy. In terms of theoretical aspects, Guan et al. [98] and Zhao et al. [99] theoretically explained the fluid drag reduction mechanism of a superhydrophobic surface using molecular dynamics and large eddy simulation turbulence models. The results showed that due to the existence of a plastron on the superhydrophobic surface, wall slip behavior occurred when the liquid flowed through the surface, resulting in a non-zero fluid velocity on the wall, and the wall slip velocity was proportional to the tangential shear stress of the solid–liquid interface.

Although the superhydrophobic surface has a high application prospect in the field of marine engineering due to its good fluid drag reduction performance, and the construction problem of a hull with a large surface area and irregular shape can be solved by the spraying method at present, the influence of the environment required for spraying and the cost of preparing the superhydrophobic material on its practical application need to be further studied. In addition, the plastron on the superhydrophobic surface becomes unstable and even disappears under the impact of high-speed water, which leads to a great reduction in its drag reduction effect. Therefore, maintaining a plastron for a long time is another problem that needs to be considered.

### 4.5. Application in Anti-Fouling

Marine fouling refers to marine attached organisms, such as animals, plants, or microorganisms, that attach to underwater surfaces, such as ship hulls, offshore structures, and marine equipment [100]. This fouling leads to increased drag and reduced fuel efficiency, which are counterproductive to the pursuit of carbon neutrality. The extracellular polymeric substances produced by microorganisms in the process of metabolic growth also induce corrosion. Moreover, creatures adhering to ship hulls can traverse international waters, reach local marine ecosystems devoid of their natural predators, and potentially trigger ecological upheavals [101].

The formation of marine fouling can be roughly divided into four stages: formation of an organic conditioning film, formation of a biological film, adhesion of macrofouling larvae, and formation of macrofouling [5]. In the early stage of a marine fouling event, an organic conditioning film composed of proteins, proteoglycans, and polysaccharides is produced by microbial communities. Planktonic bacteria and macrofouling larvae settle within hours of the formation of molecular films, especially in warm, nutrient-rich, productive waters. About a week later, microbial communities composed of bacteria, single-celled microalgae, and cyanobacteria are adsorbed on the underwater surfaces through an organic conditioning film, forming a biological film. Subsequently, protozoans and macroalgal zoospores begin to appear on the surface because of the nutrients provided by different microbial metabolites. Finally, soft and hard biofoulers, such as sponges, mussels, oysters, and barnacles, which feed on microbial communities, protozoa, and macroalgal zoospores, begin to appear on the surface and adsorb through their secretions. However, the actual process of marine fouling is very complicated and is mainly related to the species and quantity of fouling organisms in the seawater environment.
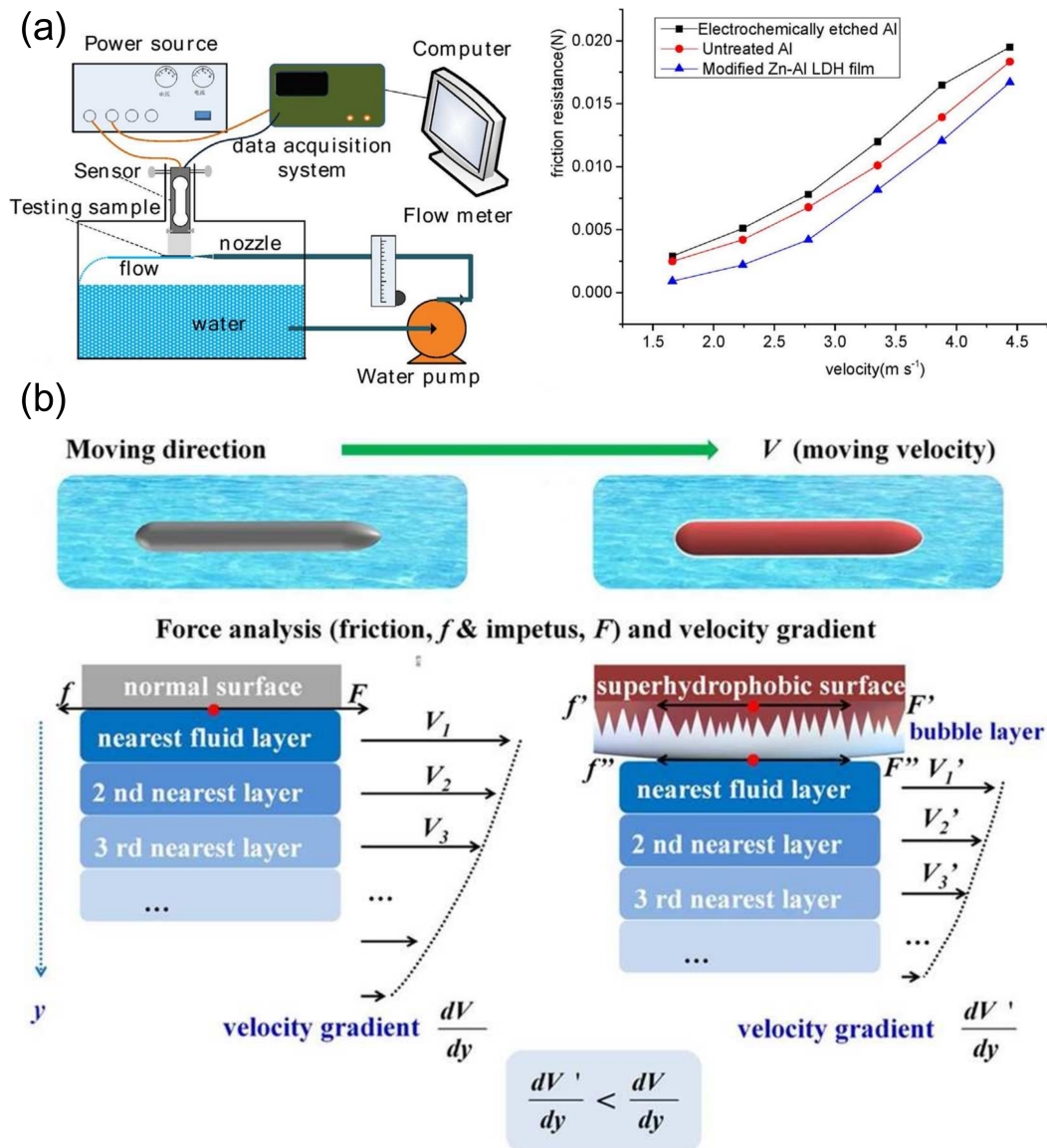
**Figure 13.** Drag reduction test: (**a**) Schematic of the frictional measurement and friction drag versus the velocity of the water flowing over surfaces with different adhesion properties [92]; (**b**) Drag-reducing mechanism of the superhydrophobic coatings. Flow conditions of the boundary layer for normal and superhydrophobic submarine models [96].

Thus, the focus of marine anti-fouling is to decrease the attachment and adhesion of these microbial communities. The nano-column [102] and plastron [103] in the binary micro-nano structure of the superhydrophobic surface and the antibacterial nanoparticle [104] in the superhydrophobic surface can effectively prevent surface pollution by microorganisms and bacteria. Therefore, superhydrophobic surfaces also have great applications in anti-fouling in the field of marine engineering.

Javad et al. [105] prepared a superhydrophobic surface by adding silver phosphate nanoparticles in polyvinyl chloride (PVC) films, and the bacterial adhesion experiments showed that the adhesion of *Staphylococcus aureus* and *Escherichia coli* was 98.8% and 98.9% less than that of pure PVC film, respectively. Bruzaud [106] fabricated a superhydrophobic surface of monomer fluorocarbon (EDOT-F4) on the surface of AISI316 stainless steel by electrodeposition and found that higher electrodeposited voltages can obtain a larger surface contact angle and sliding contact angle. The prepared superhydrophobic surface can effectively reduce the growth and adhesion of pseudomonas aeruginosa and listeria, as

shown in Figure 14a. However, due to the high ecological environment requirements in the marine field, it is particularly important to develop environmentally friendly antibacterial superhydrophobic surfaces. Zhang et al. [107] prepared a fluorine-free coating with anti-fouling and anti-microorganism properties by spraying a mixture of bisphenol A diglycidyl ether (BADGE), 1,3 dimethyl-disiloxane (TMDS), polydimethyl-siloxane (PDMS), and methyl-anthranilobenzoate (MA). Compared with the naked samples, the growth inhibition rates of *Escherichia coli*, *Staphylococcus aureus*, and penicillium were 96.2%, 92.5%, and 96.5%, respectively, as shown in Figure 14b. Selim et al. [108] prepared a marine fouling release (FR) coating of PDMS/SiC nanowire composites for ship hulls, and performed a 3-month field test in natural seawater in a tropical area. The results showed excellent fouling prevention, as shown in Figure 14c. Rasitha et al. [109] also performed a 120 h exposure test in the seawater bacterial consortium of three different superhydrophobic coatings on Al, Cr Mo, and Ti. The results showed that the SHP Al surface had the least bacterial attachment among the three SHP surfaces due to its surface morphology and chemical nature.

The anti-microorganism properties of the above-prepared superhydrophobic surfaces were mainly achieved by preventing the adhesion of microorganisms. In addition, in order to further improve the anti-fouling properties of the superhy-drophobic surface, some kinds of bactericidal substances were added to the surface. Examples include $TiO_2$ [104], ZnO [110], and $Ag^+$ [111]. These kinds of superhydrophobic surfaces mainly use the oxidation−reduction or catalytic action of these substances to generate atomic oxygen with strong oxidation to destroy the cell structure of the microorganism and bacteria to achieve the anti-fouling effect. Wang et al. [112] firstly fabricated ZnO nanowires on 304 stainless steel surfaces by laser etching and hydrothermal methods. After silane treatment, a superhydrophobic surface with a contact angle of 152° and a rolling angle of 7.3° was prepared, which reduced the adhesion to E. coli by more than 95%, and the ZnO nanowire on the surface significantly improved the anti-fouling properties. Manivasagam et al. [113] found that the superhydrophobic surface prepared by means of thermochemical treatment and silane modification on the surface of titanium metal can reduce bacteria cell adhesion significantly (>90%) and prevent biofilm formation. However, for the hull, due to the repair interval of up to 2–3 years, guaranteeing the effectiveness of the superhydrophobic surface or ensuring the durability of the effective bactericidal substances in the coating is an urgent issue to be considered.

### 4.6. Application in Anti-Icing

In a low-temperature environment, droplets are easy to condense and freeze on a solid surface, resulting in the entire device being covered by ice and affecting its performance. Examples include deck anchor winches, satellite antennae, and cranes on arctic sailing ships or marine engineering equipment operating in ice areas. Due to the low adhesion and low surface energy of the superhydrophobic surface, the droplets can easily roll or bounce on the surface, resulting in the droplets leaving the superhydrophobic surface before the formation of the ice core, thereby reducing the contact time between the droplets and the interface, delaying the icing time, and achieving the purpose of anti-icing [114–116].

Qi et al. [117] firstly obtained the microstructure on the surface of polystyrene acrylonitrile resin by etching method and then sprayed the hexamethyldisilazane-treated nano-$SiO_2$ particles to prepare the superhydrophobic surface. The results showed that the maximum freezing delay time of the droplets on the superhydrophobic surface was 97 min, which was 16 times that of the original surface, as shown in Figure 15a. The superhydrophobic Ni nano-cone surface prepared by electrodeposition on SUS304 stainless steel also showed good anti-icing ability [118]. However, it was found that if scratches existed on the surface, the contact area between the surface and droplets would increase, thus reducing the anti-icing ability of the surface. The superhydrophobic surface prepared by thermoplastic polyurethane (TPU) and modified silica particles (SH-$SiO_2$) [119] and fabricated by modified epoxy and micro-nano fluoropolymer particles (FP) [120] all showed good anti-icing properties. The precooling time can be extended by more than 200 times.
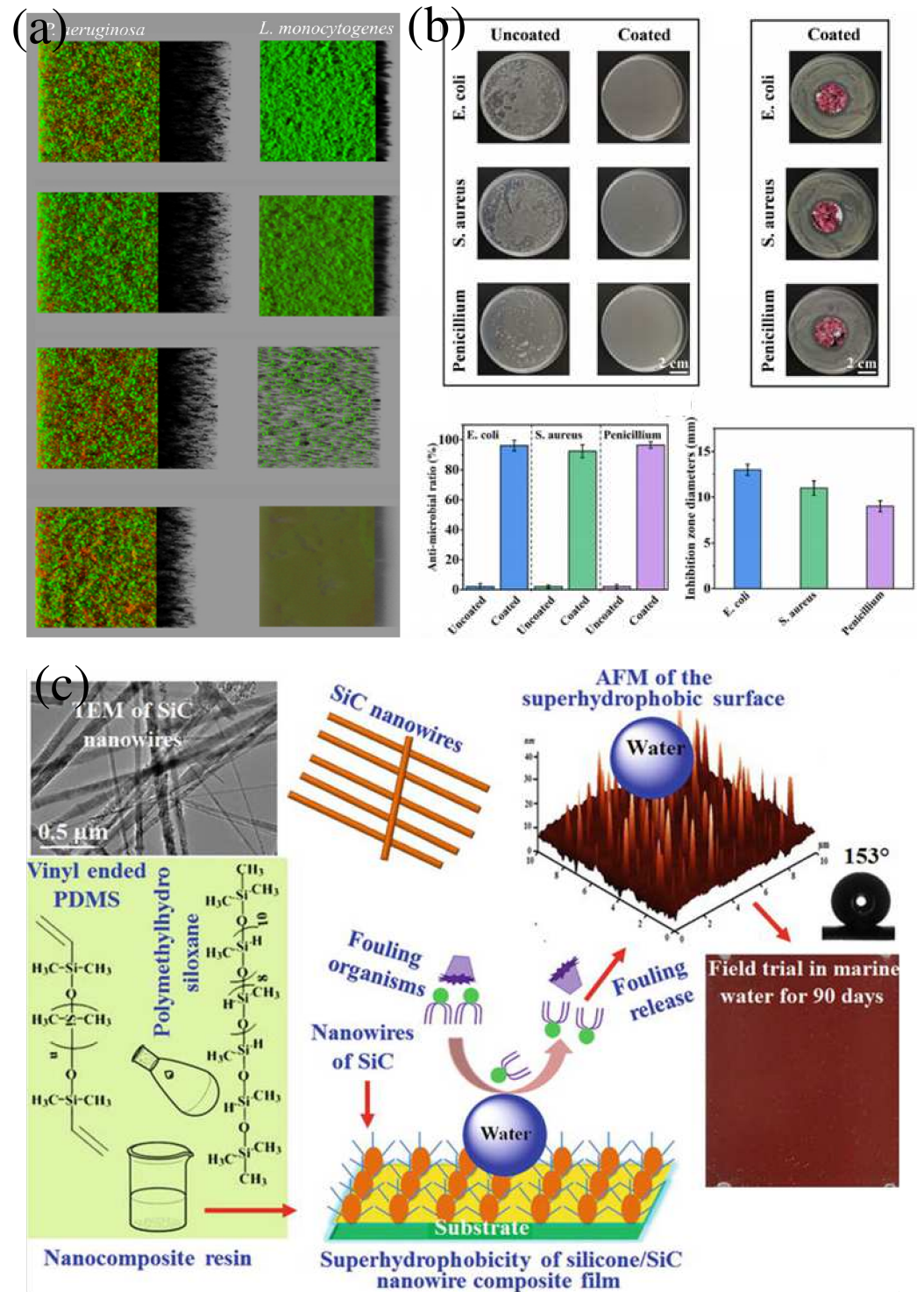
**Figure 14.** Anti-fouling test: (**a**) spatial architecture of biofilms of *P. aeruginosa* and *L. monocytogenes* [106], (**b**) statistical data of *E. coli*, *S. aureus*, and *Penicillium inhibitions* on the uncoated and coated surfaces [108], (**c**) field test in natural seawater [108].
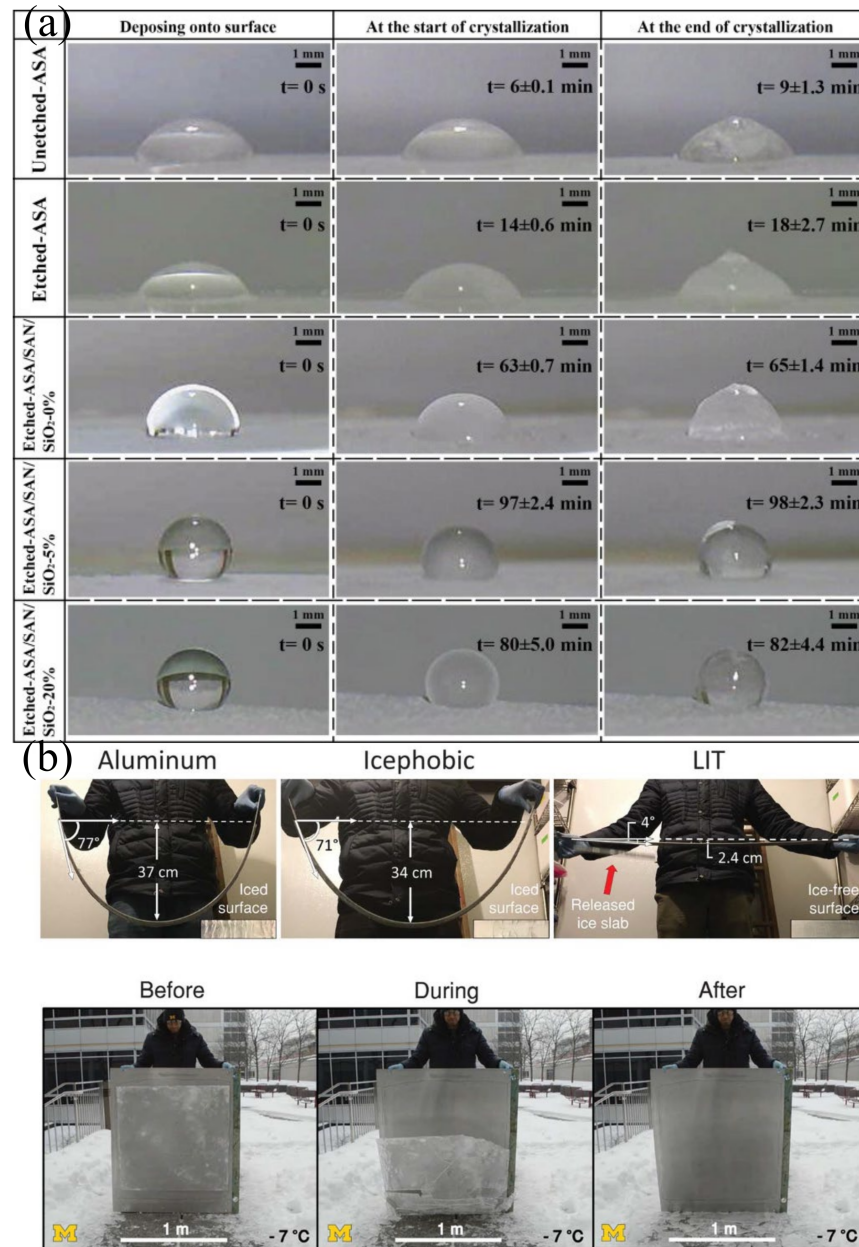
**Figure 15.** Anti-icing property test: (**a**) freezing delay time measurement [117], (**b**) ice adhesion test of large-scale aluminum beams and sheet [121].

However, it has been found that even for a superhydrophobic surface with materials of low ice adhesion strength, the force required to remove the ice from the surface increases with the surface area. Golovin et al. [121] reported a superhydrophobic surface that can de-icing on large area structures. The authors adjusted this idea from the perspective of interface toughness rather than ice adhesion and developed a superhydrophobic surface with low interfacial toughness (LIT PDMS) by adding silicone oil to polydimethylsiloxane (PDMS). The superhydrophobic surface had better de-icing performance on 1.2 m long aluminum strips and 1 square meter aluminum plate, which laid a foundation for the development of large area structure de-icing technology, as shown in Figure 15b. Some researchers have also studied the anti-icing performance of superhydrophobic surfaces at ultra-low temperatures. For example, Barthwal et al. [122] injected silicone oil into the binary micro-nano structure of a surface to prepare a superhydrophobic surface, which showed low ice adhesion strength and high recycling durability at −25 °C. Moreover, the

superhydrophobic surface prepared by grafting polyelectrolyte hydrogel onto PDMS can keep droplets unfrozen for 4800 s at $-28$ °C [123].

However, for ships navigating icy areas or production platforms, the devices onboard must work at low temperatures (below $-25$ °C) for a long time. Although the surface ice layer can fall off due to the existence of a superhydrophobic surface, the binary micro-nano structure on the surface can still be penetrated by droplets, and ice nucleation will occur under such conditions, resulting in interlock between the ice and the surface, and higher ice adhesion strength. Furthermore, the falling off of the ice layer also causes damage to the micro-nano structures of the surface. Therefore, the preparation of superhydrophobic surfaces with long-term low-temperature resistance and high surface structural strength are key problems that need to be solved for practical applications.

### 4.7. Application in Oil/Water Separation

Oil leakage has caused an extremely serious impact on the marine ecological balance. Therefore, the collection of dirty oil and oil/water separation in the marine environment are important problems that need to be solved urgently. When superhydrophobic materials (most of which are superlipophilic materials) were applied to the filter mesh, the superhydrophobic/superlipophilic mesh showed better oil/water separation performance, and the oil/water separation efficiency could reach up to 97%, as shown in Figure 16a [124,125]. It is believed that when the oil/water mixture passes through the superhydropho-bic/superlipophilic mesh, the oil is easily adsorbed and spread by the mesh, while the water is intercepted outside the mesh. When the oil in the mesh reaches saturation, it will drop under the action of gravity, thus achieving the purpose of oil/water separation [126].

Chen et al. [127] first deposited nano $SiO_2$ particles on the surface of stainless steel mesh and copper mesh by electrospray method and then modified them with dode-cyltrimethoxysilane to prepare superhydrophobic/superlipophilic mesh, which showed good water-repellency and oil absorption abilities, as shown in Figure 16b. Oil/water separation experiments showed that the separation efficiency for heavy oil and light oil was as high as 99% and reached 95% under high oil flow rates. Moreover, the prepared superhydrophobic/superlipophilic mesh can work under high/low temperatures or in saline solutions. Rosin acid and $SiO_2$ have been used to modify cotton fabric to prepare fluorine-free and environmentally friendly superhydrophobic coatings, which can be effective in separating oil-in-water and oil-in-water emulsions [128]. Sow et al. [129] modified fly ash (FA) particles with vulcanized silica gel (RTVS) and sprayed them onto the textile to prepare the textile with oil/water separation properties. The results indicated that the mixture of diesel and water with a mass ratio of 1:1 could be highly separated under gravity. After repeating this separation process for 10 cycles, the separation efficiency remained greater than 99%, as shown in Figure 16c. In addition, researchers [130] have prepared molecular membranes that can convert between superhydrophobic/superlipophilic and superhydrophilic/superlipophobic properties, which can be modified as needed to obtain excellent oil resistance and high separation efficiency, as shown in Figure 16d.

However, it was also found that the superhydrophobic/superlipophilic materials were easily contaminated by adsorbed oil, leading to a decline in the oil/water separation efficiency after prolonged usage. Therefore, the development of oil/water separation structures with high separation efficiency, environmental friendliness, and high repeat usage showed great potential for future practical industrial applications.
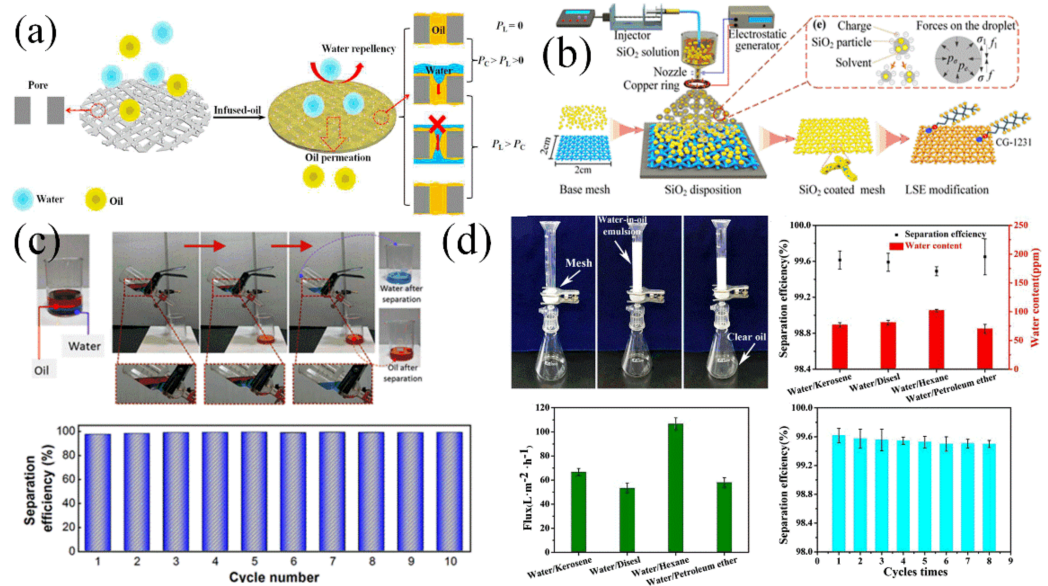
**Figure 16.** Oil/water separation property test: (**a**) schematic demonstration of the oil/water separation behavior [125], (**b**) schematic diagram of preparing superhydrophobic surface [119], (**c**) oil/water separation process [129], and (**d**) schematic demonstration of molecular films with switched hydrophilic and hydrophobic properties [128].

## 5. Future Challenges and Strategies

Due to its special surface wettability, superhydrophobic surfaces with self-cleaning, anti-corrosion, heat transfer, drag reduction, anti-microorganism, anti-icing, oil/water separation, and other properties have been used in the field of marine engineering, such as anti-corrosion paint, anti-fouling paint, drag reduction paint, and anti-icing satellite antenna. However, with the deepening of research and the development needs of other special fields, the preparation and application of high-performance and multi-functional superhydrophobic surfaces still have great constraints and great development prospects. Therefore, further research is still needed in the following aspects:

(1) In the aspect of preparation: At present, although there are many preparation methods for superhydrophobic surfaces, most of them are still based on two factors: surface binary micro/nanostructures and low surface energy. Once either of these two factors is destroyed, the superhydrophobic properties of the surface will be reduced or even lost. However, it is necessary to develop long-term stable weather-resistant superhydrophobic surfaces in humid, saline, and low-temperature marine environments. For example, shape memory polymer surfaces with superhydrophobic functionality prepared by blending bisphenol A-type epoxy resin diglycidyl ether (DGEBA), octylamine (OA), meta-xylylenediamine (MXDA), and the prepolymer of SMP [131], and self-healing superhydrophobic surfaces fabricated by applying poly(dopamine) (PDA)-coated flower-like ZnO composite particles on the self-healing polyurethane surface [132]. Furthermore, light/electrical/magnetic/thermal responsive superhydrophobic surfaces were also manufactured to maintain the damage resistance of the superhydrophobic surface. In addition, due to the high processing cost, low efficiency, and pollution of the existing materials, the preparation technology of low cost, large area, and environmentally friendly superhydrophobic surfaces should be developed to meet the needs of large-scale manufacturing in practical engineering applications.

(2) In the aspect of mechanism: For most of the research results, scholars mainly explained the mechanism from the Cassie-Baxter model and believed that the surface binary micro-nano structure and the plastron on the superhydrophobic surface were the main reasons for various superhydrophobic properties. Furthermore, molecular dynamics was used to simulate the surface wettability. For example, the effects of the order of carbon atoms and the coverage of carboxyl molecular chains on superhydrophobic properties have

been simulated [133]. The anti-wetting mechanism of fluorinated surfaces on aluminum substrates was elucidated via molecular dynamics simulations [134]. However, there is a lack of theoretical studies on the molecular dynamics between surfaces and superhydrophobic properties, such as the dynamic behavior of droplet icing and melting ice, and the phenomenon of wall slip caused by plastron. Therefore, it is necessary to investigate the molecular dynamics relationship between air or liquid and the surface structure, surface energy, surface tension, and surface adhesion force of superhydrophobic surfaces.

(3) In the aspect of test: currently, the mechanism of the superhydrophobic surface is mainly characterized by surface morphology, electrochemical testing, and other methods. However, there is still a lack of accurate and elaborate microscopic observation methods for the process of in situ observation. For example, AFM (Atomic Force Microscope) was adopted to measure the surface slip force on different superhydrophobic surfaces [135]. Laser scanning confocal microscopy was used to observe the wetting processes of the droplets on the different superhydrophobic surfaces [39]. In terms of durability testing of superhydrophobic surfaces, sandpaper friction tests, and acid, alkali, and salt immersion tests, high-temperature tests are commonly used testing methods and these tests are completed in the laboratory. However, the impact of the actual service environment on its performance is ignored, especially for irritated responsive surfaces. In addition, these testing methods do not have specific parameters or uniform standards, which makes it impossible to compare different research results. Therefore, it is necessary to enrich the microscopic observation methods, establish uniform performance test standards (tests such as mechanical abrasion, substrate adhesion, scratch resistance, erosion tests against powders, sand, chemicals, and water droplet spray [136]), and effectively simulate the actual working conditions, so as to enhance the reliability of the test and comparability of the results and promote the development of superhydrophobic surface technology.

(4) In the aspect of application: The constraints of superhydrophobic surfaces in applications are mainly related to the actual engineering environment. The self-cleaning, corrosion resistance, heat transfer, drag reduction, anti-fouling, and oil/water separation properties exhibited by superhydrophobic surfaces have been well validated in the laboratory. However, there are still many difficulties in their practical engineering applications, especially in large-scale, irregular structures, and harsh environments. Among these difficulties, poor durability is the main factor preventing superhydrophobic surfaces from appearing in mainstream applications. This is mainly reflected in the damage to the structure or chemical composition of the surface and the disappearance of the plastron on the superhydrophobic surface. Although the application of armor structures can greatly enhance the mechanical durability of superhydrophobic surfaces [39], the damage from flexible materials, such as water impact, still needs to be strengthened. There were also some fillers added to the surfaces, such as carbon nanotubes and graphene oxide [137], as hard support points on the surfaces, which could also enhance the mechanical strength of the surface. In addition, factors such as superhydrophobic surface properties, environmental and economic benefits, and commercial production should be comprehensively considered. Therefore, the development of an efficient, economical, and environmentally friendly superhydrophobic surface that can universally adapt to complex and harsh marine environments is an important research direction in the future.

(5) In the aspect of the challenges of fluoropolymer pollution. Traditional methods for preparing superhydrophobic surfaces often rely on the use of fluorinated polymers. However, the environmental impact of fluoropolymers has always been a problem; in addition to contaminating the soil, groundwater, and atmospheric ozonosphere, fluoropolymers can also cause harm to organisms. Perfluoroalkyl chains with carbon atomic numbers greater than seven are difficult to degrade in nature and exhibit bioaccumulation and toxicity. Therefore, there is an urgent need to explore alternatives to polymers containing long perfluoroalkyl chains, such as materials with low surface energy that are not limited by the single structure of fluorine compounds.

## References

1. Young, T. An essay on the cohesion of fliuds. *Philos. Trans. R. Soc.* **1805**, *95*, 65–87. [CrossRef]
2. Kock-Yee, L. Definitions for hydrophilicity, hydrophobicity, and superhydrophobicity, getting the basics right. *J. Phys. Chem. Lett.* **2014**, *5*, 686–688.
3. Rather, A.M.; Shome, A.; Bhunia, B.K.; Panuganti, A.; Mandal, B.B.; Manna, U. Correction: Simultaneous and controlled release of two different bioactive small molecules from nature inspired single material. *J. Mater. Chem. B* **2019**, *7*, 346. [CrossRef]
4. Ferrari, M.; Benedetti, A.; Cirisano, F. Superhydrophobic Coatings from Recyclable Materials for Protection in a Real Sea Environment. *Coatings* **2019**, *9*, 303. [CrossRef]
5. Selim, M.S.; Hamouda, H.I.; Fatthallah, N.A.; Mostafae, M.S.; Higazy, S.A.; Shabana, S.; EL-Saeed, A.M.; Hao, Z. *Advanced Bioinspired Superhydrophobic Marine Antifouling Coatings. Superhydrophobic Coating-Recent Advances in Theory and Applications*; IntechOpen: London, UK, 2023.
6. Cho, E.; Chang-Jian, C.; Chen, H.; Chuang, K.; Zheng, J.; Hsiao, Y.; Lee, K.; Huang, J. Robust Multifunctional superhydrophobic coatings with enhanced water/oil separation, self-cleaning, anti-corrosion, and anti-biological adhesion. *Chem. Eng. J.* **2017**, *314*, 347–357. [CrossRef]
7. Hsu, C.; Nazari, M.H.; Li, Q.; Shi, X. Enhancing degradation and corrosion resistance of AZ31 magnesium alloy through hydrophobic coating. *Mater. Chem. Phys.* **2019**, *225*, 426–432. [CrossRef]
8. Truesdell, R.; Mammoli, A.; Vorobieff, P.; van Swol, F.; Brinker, C.J. Drag reduction on a patterned superhydrophobic surface. *Phys. Rev. Lett.* **2006**, *4*, 97. [CrossRef]
9. Farhadi, S.; Farzaneh, M.; Kulinich, S.A. Anti-icing performance of superhydrophobic surfaces. *Appl. Surf. Sci.* **2011**, *257*, 6264–6269. [CrossRef]
10. Rather, M.; Jana, N.; Hazarika, P.; Manna, U. Sustainable polymeric material for the facile and repetitive removal of oil-spills through the complementary use of both selective-absorption and active-filtration processes. *J. Mater. Chem. A Mater. Energy Sustain.* **2017**, *5*, 23339–23348. [CrossRef]
11. Rather, M.; Manna, U. Stretchable and durable superhydrophobicity that acts both in air and under oil. *J. Mater. Chem. A Mater. Energy Sustain.* **2017**, *5*, 15208–15216. [CrossRef]
12. Barthlott, W.; Neinhuis, C. Purity of the sacred lotus, or escape from contamination in biological surfaces. *Planta* **1997**, *202*, 1–8. [CrossRef]
13. Neinhuis, C.; Barthlott, W. Characterization and distribution of water-repellent, self-cleaning plant surfaces. *Ann. Bot.* **1997**, *79*, 667–677. [CrossRef]
14. Barthlott, W.; Schimmel, T.; Wiersch, S.; Koch, K.; Brede, M.; Barczewski, M.; Walheim, S.; Weis, A.; Kaltenmaier, A.; Leder, A.; et al. The salvinia paradox, superhydrophobic surfaces with hydrophilic pins for air retention under water. *Adv. Mater.* **2010**, *22*, 2325–2328. [CrossRef] [PubMed]
15. Gao, X.; Jiang, L. Water-repellent legs of water striders. *Nature* **2004**, *432*, 7013–7036. [CrossRef]
16. Wang, S.; Yang, Z.; Guo, G.; Wang, J.; Wu, J.; Yang, S.; Jiang, L. Icephobicity of penguins spheniscus humboldti and an artificial replica of penguin feather with air-infused hierarchical rough structures. *J. Phys. Chem. C* **2016**, *120*, 15923–15929. [CrossRef]
17. Chen, H.; Ran, T.; Gan, Y.; Zhou, J.; Zhang, Y.; Zhang, L.; Zhang, D.; Jiang, L. Ultrafast water harvesting and transport in hierarchical microchannels. *Nat. Mater.* **2018**, *17*, 935–942. [CrossRef]
18. Bixler, G.D.; Bhushan, B. Fluid drag reduction with shark-skin riblet inspired microstructured surfaces. *Adv. Funct. Mater.* **2013**, *23*, 4507–4528. [CrossRef]
19. Luo, Y.; Zhang, D.; Xu, X.; Green, L. Precise cutting microstructured superhydrophobic surface. *Surf. Eng.* **2016**, *32*, 119–124. [CrossRef]

20. Zhang, B.; Hu, X.; Zhu, Q.; Wang, X.; Zhao, X.; Sun, C.; Li, Y.; Hou, B. Controllable dianthus caryophyllus-like superhydrophilic/superhydrophobic hierarchical structure based on self-congregated nanowires for corrosion inhibition and bio-fouling mitigation. *Chem. Eng. J.* **2017**, *312*, 317–327. [CrossRef]

21. Choi, J.; Kwon, J.; Lee, C.; Bae, K.; Sohn, S.; Kim, H. Optimization of super-hydrophobic property by two-step surface modification. *J. Nanosci. Nanotechnol.* **2019**, *19*, 7192–7197. [CrossRef]

22. Peng, S.; Deng, W. A simple method to prepare superamphiphobic aluminum surface with excellent stability. *Colloids Surf. A Physicochem. Eng. Asp.* **2015**, *481*, 143–150. [CrossRef]

23. Sun, R.; Zhao, J.; Li, Z.; Qin, N.; Mo, J.; Pan, Y.; Luo, D. Robust superhydrophobic aluminum alloy surfaces with anti-icing ability, thermostability, and mechanical durability. *Prog. Org. Coat.* **2020**, *147*, 105745. [CrossRef]

24. Fu, J.; Sun, Y.; Ji, Y.; Zhang, J. Fabrication of robust ceramic based superhydrophobic coating on aluminum substrate via plasma electrolytic oxidation and chemical vapor deposition methods. *J. Mater. Process. Technol.* **2022**, *306*, 117641. [CrossRef]

25. Shen, W.; Zhang, Z.; Xu, K.; Zhu, H.; Liu, Y.; Wu, Y.; Yang, S. Reproducible PDMS flexible superhydrophobic films: A method utilizing picosecond laser-etched templates. *Prog. Org. Coat.* **2024**, *189*, 108344. [CrossRef]

26. Chen, T.L.; Huang, C.Y.; Xie, Y.T.; Chiang, Y.Y.; Chen, Y.M.; Hsueh, H.Y. Bioinspired Durable Superhydrophobic Surface from Hierarchically Wrinkled Nanoporous Polymer. *ACS Appl. Mater. Interfaces* **2019**, *11*, 40875–40885. [CrossRef]

27. Rasitha, T.P.; Vanithakumari, S.C.; Krishna, D.N.G.; George, R.P.; Srinivasan, R.; Philip, J. Facile fabrication of robust superhydrophobic aluminum surfaces with enhanced corrosion protection and antifouling properties. *Prog. Org. Coat.* **2022**, *162*, 106560. [CrossRef]

28. ECHA (European Chemical Agency). Candidate List of Substances of Very High Concern for Authorisation. 2013. Available online: http://echa.europa.eu/web/guest/candidate-list-table (accessed on 1 May 2014).

29. Wenzel, R.N. Resistance of solid surface to wetting by water. *Ind. Eng. Chem.* **1936**, *28*, 988–994. [CrossRef]

30. Cassie, A.B.D.; Baxter, S. Wettability of porous surfaces. *Trans. Faraday Soc.* **1944**, *40*, 546–551. [CrossRef]

31. Vu, H.H.; Nguyen, N.T.; Kashaninejad, N. Re-Entrant Microstructures for Robust Liquid Repellent Surfaces. *Adv. Mater. Technol.* **2023**, *8*, 2201836. [CrossRef]

32. Milne, A.J.B.; Amirfazli, A. The Cassie equation: How it is meant to be used. *Adv. Colloid Interface Sci.* **2012**, *170*, 48–55. [CrossRef]

33. Wang, P.; Li, C.Y.; Zhang, D. Recent advances in chemical durability and mechanical stability of superhydrophobic materials: Multi-strategy design and strengthening. *J. Mater. Sci. Technol.* **2022**, *129*, 40–69. [CrossRef]

34. Wang, J.W.; Zhang, Y.B.; He, Q. Durable and robust superhydrophobic fluororubber surface fabricated by template method with exceptional thermostability and mechanical stability. *Sep. Purif. Technol.* **2023**, *306*, 122423. [CrossRef]

35. Maghsoudi, K.; Momen, G.; Jafari, R.; Farzaneh, M. Direct replication of micro-nanostructures in the fabrication of superhydrophobic silicone rubber surfaces by compression molding. *Appl. Surf. Sci.* **2018**, *458*, 619–628. [CrossRef]

36. Yun, X.; Xiong, Z.; He, Y.; Wang, X. Superhydrophobic lotus-leaf-like surface made from reduced graphene oxide through soft-lithographic duplication. *RSC Adv.* **2020**, *10*, 5478–5486. [CrossRef]

37. Peng, P.; Ke, Q.; Zhou, G.; Tang, T. Fabrication of microcavity-array superhydrophobic surfaces using an improved template method. *J. Colloid Interface Sci.* **2013**, *395*, 326–328. [CrossRef]

38. Wang, T.; Wang, H.; Wang, T.; Xu, J.; Ke, Q. Significantly improving strength and oil-adsorption performance of regular porous polydimethylsiloxane via soft template approach. *Colloids Surf. A Physicochem. Eng. Asp.* **2019**, *572*, 10–17. [CrossRef]

39. Wang, D.; Sun, Q.; Matti, J.H.; Zhang, C.; Lin, F.; Liu, Q.; Zhu, S.; Zhou, T.; Chang, Q.; He, B.; et al. Design of robust superhydrophobic surfaces. *Nature* **2020**, *582*, 55–66. [CrossRef]

40. Kim, J.H.; Mirzaei, A.; Kim, H.W.; Kim, S.S. Facile fabrication of superhydrophobic surfaces from austenitic stainless steel (AISI 304) by chemical etching. *Appl. Surf. Sci.* **2018**, *439*, 598–604. [CrossRef]

41. Zhu, J.; Hu, X. A novel and facile fabrication of superhydrophobic surfaces on copper substrate via machined operation. *Mater. Lett.* **2017**, *190*, 115–118. [CrossRef]

42. Pou, P.; Del Val, J.; Riveiro, A.; Comesaña, R.; Arias-González, F.; Lusquiños, F.; Bountinguiza, M.; Quintero, F.; Pou, J. Laser texturing of stainless steel under different processing atmospheres, from superhydrophilic to superhydrophobic surfaces. *Appl. Surf. Sci.* **2019**, *475*, 896–905. [CrossRef]

43. Dimitrakellis, P.; Gogolides, E. Atmospheric plasma etching of polymers, a palette of applications in cleaning/ashing, pattern formation, nanotexturing and superhydrophobic surface fabrication. *Microelectron. Eng.* **2018**, *194*, 109–115. [CrossRef]

44. Zhang, B.; Guan, F.; Zhao, X.; Zhang, Y.; Li, Y.; Duan, J.; Hou, B. Micro-nano textured superhydrophobic 5083 aluminum alloy as a barrier against marine corrosion and sulfate-reducing bacteria adhesion. *J. Taiwan Inst. Chem. Eng.* **2019**, *97*, 433–440. [CrossRef]

45. Zhu, J. A novel fabrication of superhydrophobic surfaces on aluminum substrate. *Appl. Surf. Sci.* **2018**, *447*, 363–367. [CrossRef]

46. Han, J.; Wang, Z.; Zhi, A.; Li, Y.; Zhao, S.; Yan, H.; Han, Q. A smart electroplating approach to fabricate mechanically robust and fluorine-free Ni-W alloys based superhydrophobic coating on Al alloy. *Vacuum* **2023**, *217*, 112501. [CrossRef]

47. Zhang, B.; Zhu, Q.; Li, Y. Facile fluorine-free one step fabrication of superhydrophobic aluminum surface towards self-cleaning and marine anticorrosion. *Chem. Eng. J.* **2018**, *352*, 625–633. [CrossRef]

48. Li, S.; Xiang, X.; Ma, B.; Meng, X. Facile preparation of diverse alumina surface structures by anodization and superhydrophobic surfaces with tunable water droplet adhesion. *J. Alloys Compd.* **2019**, *779*, 219–228. [CrossRef]

49. Zhang, C.L.; Zhang, F.; Song, L.; Zeng, R.C.; Li, S.Q.; Han, E.H. Corrosion resistance of a superhydrophobic surface on micro-arc oxidation coated Mg-Li-Ca alloy. *J. Alloys Compd.* **2017**, *728*, 815–826. [CrossRef]

50. Cui, L.; Liu, H.; Zhang, W.; Han, Z.; Deng, M.; Zeng, R.; Li, S.; Wang, Z. Corrosion resistance of a superhydrophobic micro-arc oxidation coating on Mg-4Li-1Ca alloy. *J. Mater. Sci. Technol.* **2017**, *33*, 1263–1271. [CrossRef]

51. Chen, G.; Wang, Y.; Zou, Y.; Jia, D.; Zhou, Y. A fractal-patterned coating on titanium alloy for stable passive heat dissipation and robust superhydrophobicity. *Chem. Eng. J.* **2019**, *374*, 231–241. [CrossRef]

52. Wang, H.; Di, D.; Zhao, Y.; Yuan, R.; Zhu, Y. A multifunctional polymer composite coating assisted with pore-forming agent, preparation, superhydrophobicity and corrosion resistance. *Prog. Org. Coat.* **2019**, *132*, 370–378. [CrossRef]

53. Xie, Y.; Xiong, W.; Kareem, S.; Qiu, C.; Hu, Y.; Parkin, I.P.; Wang, S.; Wang, H.; Chen, J.; Li, L.; et al. Robust superamphiphobic coatings with gradient and hierarchical architecture and excellent anti-flashover performances. *Nano Res.* **2022**, *15*, 7565–7576. [CrossRef]

54. Xin, L.; Li, H.; Gao, J.; Wang, Z.; Zhou, K.; Yu, S. Large-scale fabrication of decoupling coatings with promising robustness and superhydrophobicity for antifouling, drag reduction, and organic photodegradation. *Friction* **2023**, *11*, 716–736. [CrossRef]

55. Li, Z.; Cao, M.; Li, P.; Zhao, Y.; Bai, H.; Wu, Y.; Jiang, L. Surface-embedding of functional micro-nanoparticles for achieving versatile superhydrophobic interfaces. *Matter* **2019**, *1*, 661–673. [CrossRef]

56. Raimondo, M.; Veronesi, F.; Boveri, G.; Motta, A.; Zanoni, R. Superhydrophobic properties induced by sol-gel routes on copper surfaces. *Appl. Surf. Sci.* **2017**, *422*, 1022–1029. [CrossRef]

57. Cui, M.; Xu, C.; Shen, Y.; Tian, H.; Feng, H.; Li, J. Electrospinning superhydrophobic nanofibrous poly(vinylidene fluoride)/stearic acid coatings with excellent corrosion resistance. *Thin Solid Film.* **2018**, *657*, 88–94. [CrossRef]

58. Xiang, Y.; Huang, S.; Huang, T.Y.; Dong, A.; Duan, H. Superrepellency of underwater hierarchical structures on salvinia leaf. *Proc. Natl. Acad. Sci. USA* **2020**, *117*, 2282–2287. [CrossRef]

59. Wei, Z.; Zhang, F.; He, Q.; Dai, F. Preparation of a superhydrophobic surface by a one-step powder pressing method with liquid silicone rubber as the carrier. *ACS Omega* **2023**, *8*, 8548–8556. [CrossRef]

60. Jang, N.S.; Ha, S.H.; Kim, K.H.; Kim, J.M. Facile one-step photopatterning of hierarchical polymer structures for highly transparent, flexible superhydrophobic films. *Prog. Org. Coat.* **2019**, *130*, 24–30. [CrossRef]

61. Rather, M.; Manna, U. Facile Synthesis of Tunable and Durable Bulk Superhydrophobic Material from Amine "Reactive" Polymeric Gel. *Chem. Mater.* **2016**, *28*, 8689–8869. [CrossRef]

62. Vazirinasab, E.; Jafari, R.; Momen, G. Application of superhydrophobic coatings as a corrosion barrier, a review. *Surf. Coat. Technol.* **2019**, *375*, 100–111. [CrossRef]

63. Qian, S.; Chen, Q.; Liu, J.; Hu, C.; Hu, Y.; Yang, L.; Zhou, X.; Hong, Y. Facile fabrication of environmentally friendly bio-based superhydrophobic surfaces via UV-polymerization for self-cleaning and high efficient oil/water separation. *Prog. Org. Coat. Int. Rev. J.* **2019**, *137*, 105346.

64. Kumar, A.; Gogoi, B. Development of durable self-cleaning superhydrophobic coatings for aluminium surfaces via chemical etching method. *Tribol. Int.* **2018**, *122*, 114–118. [CrossRef]

65. Bai, X.; Yang, Q.; Fang, Y.; Zhang, J.; Yong, J.; Hou, X.; Chen, F. Superhydrophobicity-memory surfaces prepared by a femtosecond laser. *Chem. Eng. J.* **2019**, *383*, 123143. [CrossRef]

66. Wang, L.; Cui, P.; Bi, Z.; Wang, C.; Zhou, B.; Zheng, L.; Niu, H.; Wang, D.; Li, Q. Superhydrophobic ultra-high molecular weight polyethylene porous material with self-cleaning ability, long-term stability, and high durability. *Surf. Coat. Technol.* **2022**, *446*, 128792. [CrossRef]

67. Wang, C.; Tian, F.; Zhang, X. Feasible fabrication of durable superhydrophobic SiO$_2$ coatings with translucency and self-cleaning performance. *Mater. Res. Express* **2020**, *7*, 106403. [CrossRef]

68. Fu, J.; Sun, Y.; Wang, J.; Zhang, H.; Zhang, J.; Ji, Y. Fabrication of fluorine-free superhydrophobic surface on aluminum substrate for corrosion protection and drag reduction. *J. Mar. Sci. Eng.* **2023**, *11*, 520. [CrossRef]

69. Wang, J.; Wang, L.; Sun, N.; Tierney, R.; Li, H.; Corsetti, M.; Williams, L.; Wong, P.; Wong, T. Viscoelastic solid-repellent coatings for extreme water saving and global sanitation. *Nat. Sustain.* **2019**, *2*, 1097–1105. [CrossRef]

70. Su, B.; Li, Y.; Wu, Z.; Shi, C.; Xu, Y.; Chen, A.; Yan, C.; Shi, Y. Abrasion-resistant super-slippery flush toilets fabricated by a selective laser sintering 3D printing technology. *SSRN Electron. J.* **2022**. [CrossRef]

71. Bi, P.; Li, H.; Zhao, G.; Ran, M.; Cao, L.; Guo, H.; Xue, Y. Robust super-hydrophobic coating prepared by electrochemical surface engineering for corrosion protection. *Coatings* **2019**, *9*, 452. [CrossRef]

72. Li, X.; Zhang, Q.; Guo, Z.; Shi, T.; Yu, J.; Tang, M.; Huang, X. Fabrication of superhydrophobic surface with improved corrosionin-hibition on 6061 aluminum alloy substrate. *Appl. Surf. Sci.* **2015**, *342*, 76–83. [CrossRef]

73. Li, D.; Wang, H.; Luo, D.; Liu, Y.; Han, Z.; Ren, L. Corrosion resistance controllable of biomimetic superhydrophobic microstructured magnesium alloy by controlled adhesion. *Surf. Coat. Technol.* **2018**, *347*, 173–180. [CrossRef]

74. Ma, Q.; Tong, Z.; Wang, W.; Dong, G. Fabricating robust and repairable superhydrophobic surface on carbon steel by nanosecond laser texturing for corrosion protection. *Appl. Surf. Sci.* **2018**, *455*, 748–757. [CrossRef]

75. Zhang, B.; Li, J.; Zhao, X.; Hu, X.; Yang, L.; Wang, N.; Li, Y.; Hou, B. Biomimetic one step fabrication of manganese stearate superhydrophobic surface as an efficient barrier against marine corrosion and Chlorella vulgaris-induced biofouling. *Chem. Eng. J.* **2016**, *306*, 441–451. [CrossRef]

76. Han, B.; Wang, H.; Yuan, S.; Li, Y.; Zhu, Y. Durable and anti-corrosion superhydrophobic coating with bistratal structure prepared by ambient curing. *Prog. Org. Coat.* **2020**, *149*, 105922. [CrossRef]

77. Wu, S.W.; Jiang, Q.T.; Yuan, S.; Zhao, Q.K.; Liu, C.; Tang, H. Environmentally friendly expanded graphite-doped ZnO superhydrophobic coating with good corrosion resistance in marine environment. *Rare Met.* **2023**, *42*, 3075–3087. [CrossRef]

78. Jo, H.; Ahn, H.S.; Kang, S.; Kim, M.H. A study of nucleate boiling heat transfer on hydrophilic, hydrophobic and heterogeneous wetting surfaces. *Int. J. Heat Mass Transf.* **2011**, *54*, 5643–5652. [CrossRef]

79. Betz, A.R.; Jenkins, J.; Attinger, D. Boiling heat transfer on superhydrophilic, superhydrophobic, and superbiphilic surfaces. *Int. J. Heat Mass Transf.* **2013**, *57*, 733–741. [CrossRef]

80. Vakarelski, I.U.; Patankar, N.A.; Marston, J.O.; Chan, D.Y.C.; Thoroddsen, S.T. Stabilization of Leidenfrost vapour layer by textured superhydrophobic surfaces. *Nature* **2012**, *489*, 274.e7. [CrossRef]

81. Searle, M.; Emerson, P.; Crockett, J.; Maynes, D. Influence of microstructure geometry on pool boiling at superhydrophobic surfaces. *Int. J. Heat Mass Transf.* **2018**, *127*, 772–783. [CrossRef]

82. Qin, L.; Li, S.; Zhao, X.; Zhang, X. Experimental research on flow boiling characteristics of micro pin-fin arrays with different hydrophobic coatings. *Int. Commun. Heat Mass Transf.* **2021**, *126*, 105456. [CrossRef]

83. Miljkovic, N.; Enright, R.; Nam, Y.; Lopez, K.; Dou, N.; Sack, J.; Wang, E.N. Jumping-droplet-enhanced condensation on scalable superhydrophobic nanostructured surfaces. *Nano Lett.* **2013**, *13*, 179–187. [CrossRef] [PubMed]

84. Miljkovic, N.; Wang, E.N. Condensation heat transfer on superhydrophobic surfaces. *MRS Bull.* **2013**, *38*, 397–406. [CrossRef]

85. Zhang, T.Y.; Mou, L.W.; Zhang, J.Y.; Fan, L.W.; Li, J.Q. A visualized study of enhanced steam condensation heat transfer on a honeycomb-like microporous superhydrophobic surface in the presence of a non-condensable gas. *Int. J. Heat Mass Transf.* **2020**, *150*, 119352. [CrossRef]

86. Khatir, Z.; Kubiak, K.J.; Jimack, P.K.; Mathia, T.G. Dropwise condensation heat transfer process optimization on superhydrophobic surfaces using a multi-disciplinary approach. *Appl. Therm. Eng.* **2016**, *106*, 1337–1344. [CrossRef]

87. Hao, T.; Wang, K.; Chen, Y.; Ma, X.; Lan, Z.; Bai, T. Multiple bounces and oscillatory movement of a microdroplet in superhydrophobic minichannels. *Ind. Eng. Chem. Res.* **2018**, *57*, 4452–4461. [CrossRef]

88. Taghvaei, E.; Moosavi, A.; Nouri-Borujerdi, A.; Daeian, M.A.; Vafaeinejad, S. Superhydrophobic surfaces with a dual-layer micro- and nanoparticle coating for drag reduction. *Energy* **2017**, *125*, 1–10. [CrossRef]

89. Zhao, X.; Zong, Z.; Jiang, Y.; Sun, T. A numerical investigation of the mechanism of air-injection drag reduction. *Appl. Ocean Res.* **2020**, *94*, 101978. [CrossRef]

90. Mäkiharju, S.A.; Ceccio, S.L. On multi-point gas injection to form an air layer for frictional drag reduction. *Ocean. Eng.* **2018**, *147*, 206–214. [CrossRef]

91. Park, H.J.; Tasaka, Y.; Oishi, Y.; Murai, Y. Drag reduction promoted by repetitive bubble injection in turbulent channel flows. *Int. J. Multiph. Flow* **2015**, *75*, 12–25. [CrossRef]

92. Zhang, H.; Yin, L.; Liu, X.; Weng, R.; Wang, Y.; Wu, Z. Wetting behavior and drag reduction of superhydrophobic layered double hydroxides films on aluminum. *Appl. Surf. Sci.* **2016**, *380*, 178–184. [CrossRef]

93. Sun, R.; Zhao, J.; Mo, J.; Yu, N.; Zhou, Z. Study of the drag reduction performance on steel spheres with superhydrophobic ER/ZnO coating. *Mater. Sci. Eng. B* **2023**, *288*, 116144. [CrossRef]

94. Abu Rowin, W.; Hou, J.; Ghaemi, S. Turbulent channel flow over riblets with superhydrophobic coating. *Exp. Therm. Fluid Sci.* **2018**, *94*, 192–204. [CrossRef]

95. Wang, N.; Tang, L.; Cai, Y.; Tong, W.; Xiong, D. Scalable superhydrophobic coating with controllable wettability and investigations of its drag reduction. *Colloids Surf. A Physicochem. Eng. Asp.* **2018**, *555*, 290–295. [CrossRef]

96. Zhang, S.; Ouyang, X.; Li, J.; Gao, S.; Han, S.; Liu, L.; Wei, H. Underwater Drag-Reducing Effect of Superhydrophobic Submarine Model. *Langmuir* **2015**, *31*, 587–593. [CrossRef]

97. Zhao, J.; Sun, R.; Liu, C.; Mo, J. Application of ZnO/epoxy resin superhydrophobic coating for buoyancy enhancement and drag reduction. *Colloids Surf. A Physicochem. Eng. Asp.* **2022**, *651*, 129714. [CrossRef]

98. Guan, N.; Liu, Z.; Jiang, G.; Zhang, C.; Ding, N. Experimental and theoretical investigations on the flow resistance reduction and slip flow in super-hydrophobic micro tubes. *Exp. Therm. Fluid Sci.* **2015**, *69*, 45–57. [CrossRef]

99. Hao, Y.; Wong, P.L.; Mao, J.H. Solving coupled boundary slip and heat transfer EHL problem under large slide-roll ratio conditions. *Tribol. Int.* **2019**, *133*, 73–87.

100. Liu, Y.; Zhang, L.; Zhang, C.; Liu, L. Bioinspired antifouling Fe-based amorphous coating via killing-resisting dual surface modifications. *Sci. Rep.* **2022**, *12*, 819. [CrossRef]

101. Rasitha, T.P.; Krishna, N.G.; Anandkumar, B.; Vanithakumari, S.C.; Philip, J. A comprehensive review on an-ticorrosive/antifouling superhydrophobic coatings: Fabrication, assessment, applications, challenges and future perspec-tives. *Adv. Colloid Interface Sci.* **2024**, *324*, 103090. [CrossRef]

102. Mahmoodi, N.; Bazzoli, D.G.; Overton, T.W.; Mendes, P.M. Plasma Activation and its Nanoconfinement Effects Boost Surface Anti-Biofouling Performance. *Adv. Mater. Interfaces* **2023**, *10*, 2202087. [CrossRef]

103. Wang, Z.; Su, Y.; Li, Q.; Liu, Y.; She, Z.; Chen, F.; Li, L.; Zhang, X.; Zhang, P. Researching a highly anti-corrosion superhydrophobic film fabricated on AZ91D magnesium alloy and its anti-bacteria adhesion effect. *Mater. Charact.* **2015**, *99*, 200–209. [CrossRef]

104. Zhang, Y.; Chen, Y.; Wang, C.; Fan, Z.; Wang, Y. A multifunctional composite membrane with photocatalytic, self-cleaning, oil/water separation and antibacterial properties. *Nanotechnology* **2022**, *33*, 355703. [CrossRef] [PubMed]

105. Seyfi, J.; Panahi-Sarmad, M.; OraeiGhodousi, A.; Goodarzi, V.; Khonakdar, H.A.; Asefnejad, A.; Shojaei, S. Antibacterial superhydrophobic polyvinyl chloride surfaces via the improved phase separation process using silver phosphate nanoparticles. *Colloids Surf. B Biointerfaces* **2019**, *183*, 110438. [CrossRef] [PubMed]

106. Bruzaud, J.; Tarrade, J.; Celia, E.; Thierry, D.; Elisabeth, T.G.; Frédéric, G.; Jean-Marie, H.; Morgan, G.; Marie-Noëlle, B. The design of superhydrophobic stainless steel surfaces by controlling nanostructures, a key parameter to reduce the implantation of pathogenic bacteria. *Mater. Sci. Eng. C* **2017**, *73*, 40–47. [CrossRef]

107. Zhang, X.; Han, H.; Kuang, W.; Tian, H.; Wang, X.; Cheng, W. Facile fabrication of fluorine-free slippery antifouling coatings with self-cleaning and anti-microorganism properties. *J. Mater. Sci.* **2023**, *21*, 8969–8980. [CrossRef]

108. Selim, M.; Yang, H.; Wang, F.; Fatthallah, N.; Nesreen, A.; Li, X.; Li, Y.; Huang, Y. Superhydrophobic silicone/SiC nanowire composite as a fouling release coating material. *J. Coat. Technol. Res.* **2019**, *16*, 1165–1180. [CrossRef]

109. Rasitha, T.P.; Sofia, S.; Anandkumar, B.; Philip, J. Long term antifouling performance of superhydrophobic surfaces in seawater environment: Effect of substrate material, hierarchical surface feature and surface chemistry. *Colloids Surf. A Physicochem. Eng. Asp.* **2022**, *647*, 129194. [CrossRef]

110. Suryaprabha, T.; Ha, H.; Hwang, B.; Sethuraman, M.G. Self-cleaning, superhydrophobic, and antibacterial cotton fabrics with chitosan-based composite coatings. *Int. J. Biol. Macromol.* **2023**, *250*, 126217. [CrossRef]

111. Ghamari, N.; Ahmadi, R.; Sheikhzadeh, M.S.; Afshar, A. Development of PDMS/$TiO_2$/$Ag_3PO_4$ antibacterial coating on 316L/PDMS implants, evaluation of superhydrophobicity, bio-corrosion, mechanical behaviour, surface nanostructure and chemistry. *J. Mech. Behav. Biomed. Mater.* **2024**, *150*, 106315. [CrossRef]

112. Wang, B.; An, W.; Wang, L.; Jiao, L.; Zhang, H.; Song, H.; Liu, S. Superhydrophobic and antibacterial hierarchical surface fabricated by femtosecond laser. *Sustainability* **2022**, *14*, 12412. [CrossRef]

113. Manivasagam, V.K.; Perumal, G.; Arora, H.S.; Popat, K.C. Enhanced antibacterial properties on superhydrophobic micro-nano structured titanium surface. *J. Biomed. Mater. Res. A* **2022**, *110*, 1314–1328. [CrossRef] [PubMed]

114. Chen, Z.; Song, L.; Wang, Y.; Tao, H.; Liu, Z.; Wang, T.; Ye, F.; He, Y.; Lin, J. Air pocket-optimization strategy for micro/nanostructures fabricated by femtosecond laser technology for anti-icing per-formance improvement. *Appl. Surf. Sci.* **2024**, *655*, 159454. [CrossRef]

115. Shen, Y.; Tao, J.; Wang, G.; Zhu, C.; Chen, H.; Jin, M.; Xie, Y. Bioinspired fabrication of hierarchical-structured superhydrophobic surfaces to understand droplet bouncing dynamics for enhancing water repellency. *J. Phys. Chem. C* **2018**, *122*, 7312–7320. [CrossRef]

116. Farokhirad, S.; Lee, T. Computational study of microparticle effect on self-propelled jumping of droplets from superhydrophobic substrates. *Int. J. Multiph. Flow* **2017**, *95*, 220–234. [CrossRef]

117. Qi, Y.; Yang, Z.; Chen, T.; Xi, Y.; Zhang, J. Fabrication of superhydrophobic surface with desirable anti-icing performance based on micro/nano-structures and organosilane groups. *Appl. Surf. Sci.* **2020**, *501*, 144165. [CrossRef]

118. Wang, Y.; Zhang, G.; He, Z.; Chen, J.; Gao, W.; Cao, P. Superhydrophobic Ni nanocone surface prepared by electrodeposition and its overall performance. *Surf. Coat. Technol.* **2023**, *464*, 129548. [CrossRef]

119. Shi, J.; Zhang, B.; Zhou, X.; Liu, R.; Hu, J.; Zheng, H.; Chen, Z. An abrasion resistant TPU/SH–$SiO_2$ superhydrophobic coating for anti-icing and anti-corrosion applications. *J. Renew. Mater.* **2022**, *10*, 1239–1255. [CrossRef]

120. Zeng, D.; Li, Y.; Huan, D.; Liu, H.; Wang, J. Robust epoxy-modified superhydrophobic coating for aircraft anti-icing systems. *Colloids Surf. A Physicochem. Eng. Asp.* **2021**, *3*, 127377. [CrossRef]

121. Golovin, K.; Dhyani, A.; Thouless, M.D.; Tuteja, A. Low-interfacial toughness materials for effective large-scale deicing. *Science* **2019**, *364*, 371–375. [CrossRef]

122. Barthwal, S.; Lee, B.; Lim, S.-H. Fabrication of robust and durable slippery anti-icing coating on textured superhydrophobic aluminum surfaces with infused silicone oil. *Appl. Surf. Sci.* **2019**, *496*, 143677. [CrossRef]

123. He, Z.; Wu, C.; Hua, M.; Wu, S.; Wu, D.; Zhu, X.; Wang, J.; He, X. Bioinspired multifunctional anti-icing hydrogel. *Matter* **2020**, *2*, 723–734. [CrossRef]

124. Xie, A.; Cui, J.; Chen, Y.; Lang, J.; Li, C.; Yan, Y.; Dai, J. One-step facile fabrication of sustainable cellulose membrane with superhydrophobicity via a sol-gel strategy for efficient oil/water separation. *Surf. Coat. Technol.* **2019**, *361*, 19–26. [CrossRef]

125. Li, H.; Zhu, G.; Shen, Y.; Han, Z.; Zhang, J.; Li, J. Robust superhydrophobic attapulgite meshes for effective separation of water-in-oil emulsions. *J. Colloid Interface Sci.* **2019**, *557*, 84–93. [CrossRef]

126. Liu, P.; Niu, L.; Tao, X.; Li, X.; Zhang, Z. Facile preparation of superhydrophobic quartz sands with micro-nano-molecule hierarchical structure for controlling the permeability of oil and water phase. *Colloids Surf. A Physicochem. Eng. Asp.* **2019**, *569*, 1–9. [CrossRef]

127. Chen, F.; Hao, S.; Huang, S.; Lu, Y. Nanoscale $SiO_2$-coated superhydrophobic meshes via electro-spray deposition for oil-water separation. *Powder Technol.* **2020**, *373*, 82–92. [CrossRef]

128. Chen, C.; Li, Z.; Hu, Y.; Huang, Q.; Li, X.; Qing, Y.; Wu, Y. Rosin acid and $SiO_2$ modified cotton fabric to prepare fluorine-free durable superhydrophobic coating for oil-water separation. *J. Hazard. Mater.* **2022**, *440*, 129797. [CrossRef]

129. Sow, P.; Singhal, R.; Sahoo, P.; Radhakanth, S. Fabricating low-cost, robust superhydrophobic coatings with re-entrant topology for self-cleaning, corrosion inhibition, and oil-water separation. *J. Colloid Interface Sci.* **2021**, *600*, 358–372. [CrossRef]

130. Wu, M.; An, N.; Li, Y.; Sun, J. Layer-by-layer assembly of fluorine-free polyelectrolyte-surfactant complexes for the fabrication of self-healing superhydrophobic films. *Langmuir* **2016**, *32*, 12361–12369. [CrossRef]

131. Cheng, Z.; Zhang, D.; Tong, L.; Lai, H.; Zhang, E.; Kang, H.; Wang, Y.; Liu, P.; Liu, Y.; Du, Y.; et al. Superhydrophobic Shape Memory Polymer Arrays with Switchable Isotropic/Anisotropic Wetting. *Adv. Funct. Mater.* **2017**, *28*, 1705002. [CrossRef]
132. Li, C.Y.; Wang, P.; Zhang, D.; Wang, S. Near-Infrared Responsive Smart Superhydrophobic Coating with Self-Healing and Robustness Enhanced by Disulfide-Bonded Polyurethane. *ACS Appl. Mater. Interfaces* **2022**, *14*, 45988–46000. [CrossRef]
133. Yan, J.; Liu, G.; Wang, T.; Zhao, J.; Ding, Y.; Chen, N. Analysis of superhydrophobic material performance based on molecular dynamics simulations. *Surf. Eng.* **2016**, *32*, 147–156. [CrossRef]
134. He, X.; Lou, T.; Cao, P.; Bai, X.; Yuan, C.; Wang, C.; Neville, A. Experimental and molecular dynamics simulation study of chemically stable superhydrophobic surfaces. *Surf. Coat. Technol.* **2021**, *418*, 127236. [CrossRef]
135. Bhushan, B.; Wang, Y.; Maali, A. Boundary Slip Study on Hydrophilic, Hydrophobic, and Superhydrophobic Sur-faces with Dynamic Atomic Force Microscopy. *Langmuir* **2009**, *25*, 8117–8121. [CrossRef]
136. Erbil, Y. Practical Applications of Superhydrophobic Materials and Coatings: Problems and Perspectives. *Langmuir* **2020**, *36*, 2493–2509. [CrossRef]
137. Yang, H.; Zhao, J.; Alodhayb, A.; Ma, G. Carbon-based nanotube and graphene thermal stable materials generated via surface oxidation and chemical modification. *Inorg. Chem. Commun.* **2024**, *160*, 111972. [CrossRef]